Correspondence to:
M. Basilici,
matteo.basilici@unicam.it

Space and Time Variability of Detachment- Versus Ramp-Dominated Thrusting: Insights From the Outer Albanides

S. Mazzoli[1] , **M. Basilici[1]** , **V. Spina[2]** , **P. P. Pierantoni[1]** , and **E. Tondi[1,3]**

[1]School of Science and Technology—Geology Division, University of Camerino, Camerino, Italy, [2]Total Upstream Nigeria Limited, lgos, Nigeria, [3]National Institute of Geophysics and Volcanology (INGV), Rome, Italy

Abstract Despite their markedly different structural setting, the northern and southern outer Albanides share a common tectonic evolution from detachment-dominated to ramp-dominated, basement-involved thrusting. The former process (mainly Oligocene to Miocene) is essentially related with the occurrence of a thick décollement level represented by Triassic evaporites, while the latter involves basement ramps splaying out from a middle crustal décollement. As this weak crustal layer is inherited from the Mesozoic rifting stage, the original continental margin architecture is interpreted to strongly influence subsequent convergent deformation. The profoundly different nature of the two dominant décollements in the study area controlled the structural style of the fold and thrust belt. The decoupling capacity of the upper décollement is strongly dependent on the thickness of the Triassic evaporites. Where this is significant (≫1 km; southern outer Albanides), the occurrence of such a thick incompetent layer at the base of competent carbonate units favored the development of break-thrust folds and imbrication of the sedimentary cover. Fold and thrust belt propagation was instead hindered where original stratigraphic variations resulted in a reduced thickness (≤1 km) of Triassic evaporites. On the other hand, the deeper middle crustal décollement is controlled by basement rheology. Its reactivation during plate convergence was assisted by collision-related thermal weakening of the crust. This process governed late-stage (<5 Ma) crustal-scale tectonic inversion and plays a major role in controlling present-day seismicity.

Plain Language Summary Mountain building occurs by a wide range of processes. Deformation can affect only the sedimentary cover that forms the uppermost layer of the Earth's crust, or the entire upper crust, or even the whole crust. Here we show how the mountains of Albania were formed by two main stages of deformation having profoundly different characteristics. A first stage of deformation affected the sedimentary cover alone. During this stage, which lasted for more than 30 million years, the distribution and intensity of the deformation were mainly controlled by the thickness of a weak layer (dominated by Triassic salt) located at the base of the sedimentary cover. In the last 5 million years, a second stage of deformation affected the entire upper crust, including both basement and sedimentary cover. This deeper deformation is inferred as related with the activation of a weak layer located in the middle crust and inherited from the Mesozoic rifting stage. Recent deformation of the entire upper crust eventually led to emersion and related erosion of the mountain belt. Recent basement deformation also plays a major role in the seismicity of the coastal area of Albania and adjacent offshore.

1. Introduction

Since the pioneering work by Coward (1983), a first order distinction has been commonly made in fold and thrust belts between thin-skinned and thick-skinned structural styles. These concepts have been often used to imply that the former controls deformation of detached sedimentary successions—overlying an undeformed basement—in the outer sectors of orogenic belts, while the latter is dominant in the inner portions where the basement (or metamorphic rocks) is involved in deformation. However, this notion is seriously challenged by numerous studies documenting basement-involved thrusting in the outer portions of fold and thrust belts (e.g., Berberian, 1995; Butler et al., 2004; Koshnaw et al., 2017; Lacombe & Bellahsen, 2016; Mazzoli et al., 2014; Sepehr & Cosgrove, 2004; Tavani, Parente, Puzone, et al., 2018; Vergés et al., 2011), as well as by the evidence of the coeval activation of multiple detachments within sedimentary successions and basement thrusting at depth along the same vertical (e.g., Ballard et al., 2018; Coward et al., 1999). The very equation of basement-involved

Supervision: S. Mazzoli, V. Spina
Validation: S. Mazzoli, M. Basilici, V. Spina, P. P. Pierantoni
Visualization: M. Basilici, P. P. Pierantoni
Writing – original draft: S. Mazzoli, M. Basilici
Writing – review & editing: S. Mazzoli, M. Basilici

thrusting with thick-skinned tectonics appears to be incorrect, as Coward (1983) originally indicated thick-skinned thrusting as characterizing regions "where much of the crust is involved and where the thrusts are frequently observed to become steeper downwards." Along this line, Pfiffner (2006, 2017) proposed the use of the term "basement-involved thin-skinned tectonics" for thrust systems that developed above a detachment located a few kilometers beneath the basement-cover interface, therefore resulting in stacks of basement-cored thrust sheets. According to this author, the term thick-skinned thrusting should be used for thrust faults cutting across the entire upper crust or even the whole crust. This process is characterized by warping of the basement-cover interface and generally limited continental shortening. Indeed, Butler and Mazzoli (2006) pointed out that a better definition of thick-skinned thrusting would be that the thrust system is dominated by crustal ramps, while limited displacements occur along thrust flats (located either along the basement-cover interface or within the upper part of the crystalline basement). In contrast, based on the same authors, thin-skinned thrusting is dominated by slip along major detachment levels; thrust trajectorifsdes at a very low angle imply that lower and upper crustal deformations occur at separate locations (i.e., not along the same vertical). Building upon these concepts, one could have either (Figure 1a): (i) ramp-dominated, basement-involved thrusting, or (ii) detachment-dominated, basement-involved thrusting (equivalent to Pfiffner's "basement-involved thin-skinned tectonics"). Similarly, shortening of the sedimentary cover alone could be either (iii) ramp-dominated (with limited shortening, possibly accommodated by folding and reverse faulting above a thick ductile décollement located at the basement-cover interface) or (iv) detachment-dominated (with greater shortening characterized by large "flat-on-flat" thrust segments and stacking of far-traveled thrust sheets). Model (iii) implies that the basement and underlying continental crust are homogeneously deformed by bulk coaxial strain (i.e., pure shear-dominated deformation; Butler & Mazzoli, 2006) and/or the less competent unit at the base of the sedimentary cover is deformed by non-coaxial strain (i.e., simple shear) typically accompanied by flow of incompetent material (shale or salt), a combination of these processes being most likely. On the other hand, subordinate thrust ramps are obviously present among the dominant flat segments in model (iv) as they are required to connect lower and upper detachments. Mixed models involve the independent development of detachment- and ramp-dominated structures along the same vertical (Figure 1b). Such mixed models clearly imply shortening of the sedimentary cover and of the basement/whole crust occurring at separate locations, and/or basement underthrusting and removal by continental subduction (a well-known process in the Alpine-Himalayan orogen; e.g., Chopin, 1987; Seeber et al., 1981; Pfiffner, 2017; and references therein).

At the lithosphere scale, rheological considerations predict deformation characterized by different degrees of localization, from distributed bulk strain to slip along discrete fault surfaces (Butler & Mazzoli, 2006): thrust faults would occur in the upper crust and upper mantle (brittle-frictional behavior) and would be connected by a zone of simple shear within the middle-lower crust (ductile-viscous behavior). Modes and timing of (re) activation of a middle crustal décollement in the outer portions of collisional fold and thrust belts have been recently discussed by Tavani et al. (2021). These authors pointed out a close relationship between the evolution of orogenic systems and crustal architecture (and related rheology) inherited from their former rifted continental margins (Figure 2). An early stage of collision involves the activation of a thin-skinned décollement level along which the sedimentary cover of the distal portions of the former rifted margin is detached from its basement and is emplaced onto the former necking and proximal domains. This décollement level forms in the previously thinned domain of the margin, where extension-related, syn-rift coupling between the brittle upper crust and the brittle upper mantle prevents the syn-orogenic formation of a ductile crustal layer beneath the sedimentary cover. Arrival at the convergence zone of the necking and proximal domains of the rifted margin, in which the middle crustal ductile layer is preserved, triggers the reactivation of such a ductile layer as a décollement level. This produces basement-involved thrusting in the outer zone of the orogen. As this process does not involve stacking of basement-cored thrust sheets, but rather limited shortening produced by reverse faulting, its description as a switch to "late thick-skinned deformation forelandward" (Lacombe & Bellahsen, 2016) is in line with the definition of ramp-dominated basement-involved thrusting proposed above (Figure 1). In fact, although thrusting does not involve the whole—or most—of the crust, ductile shear along the middle crustal décollement (i.e., the "flat" component of the deep thrust system) may be envisaged as being minor at the crustal scale.

Upper crustal basement ramps dominate the architecture of deep thrust systems in the outer portions of various orogens, including the Apennines (Mazzoli et al., 2014) and the Zagros Mountains (Berberian, 1995; Koshnaw et al., 2017; Tavani et al., 2020; Vergés et al., 2011), as well as the mountain belts of Oman and Taiwan (Lacombe & Bellahsen, 2016; Tavani et al., 2021; and references therein). The development of such deep thrust systems may
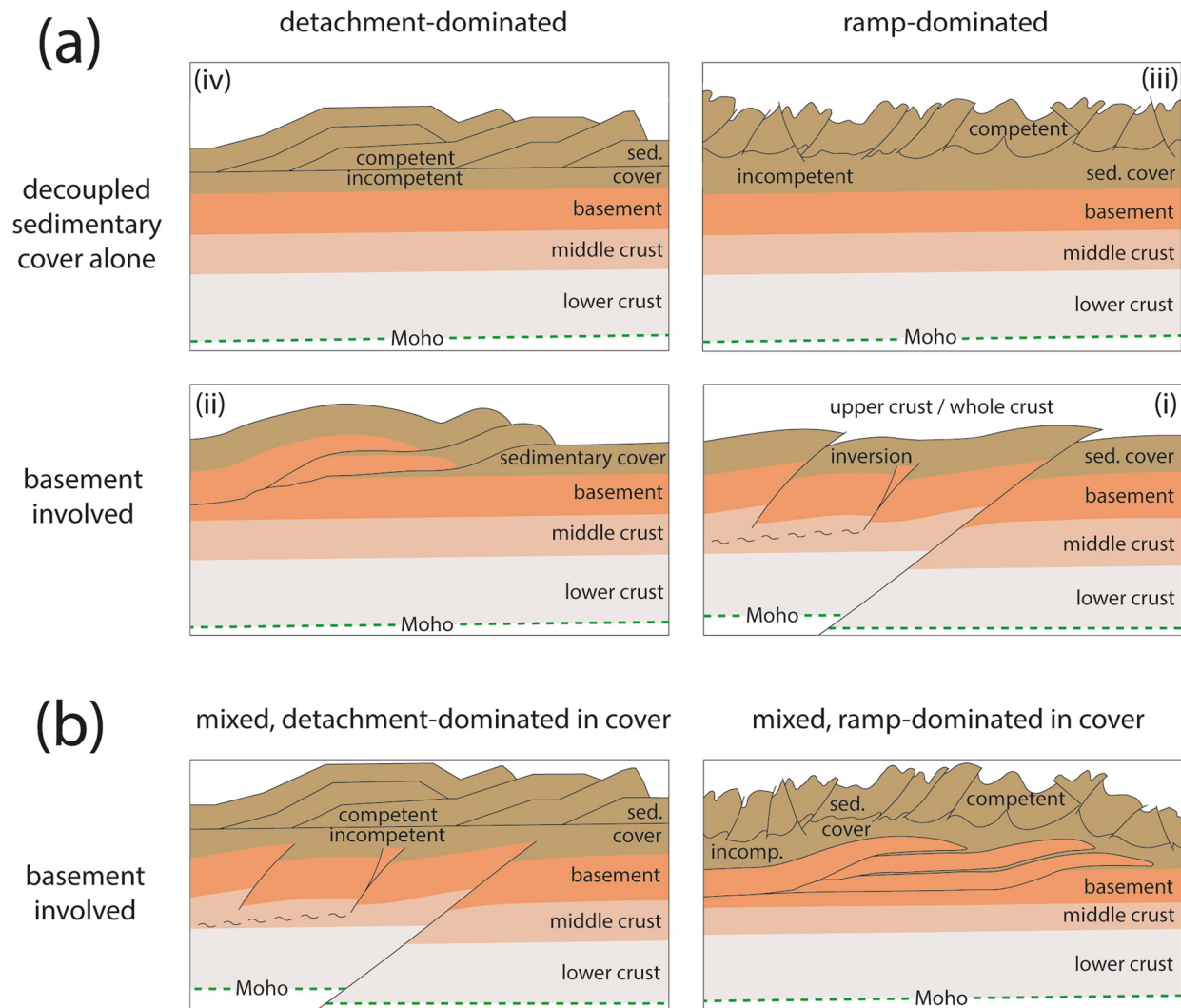
Figure 1. Cartoons showing idealized and simplified structural styles in fold and thrust belts. (a) End-member models of detachment-dominated and ramp-dominated thrusting. (b) Mixed models, characterized by the coexistence of detachment-dominated and ramp-dominated thrusting along the same vertical.

be accompanied by the reactivation of inherited extensional faults (e.g., Butler et al., 2006; Giambiagi et al., 2009; Scisciani, 2009), resulting in variable degrees of tectonic inversion. Even where pre-orogenic normal faults are not reactivated, these structures represent important mechanical discontinuities that may control the geometry of shortening-related features (Butler & Mazzoli, 2006). The interested reader is referred to Lacombe and Bellahsen (2016) for an exhaustive discussion of the combination of factors—composition, thermal state, structural inheritance—controlling lithosphere rheology and the occurrence and style (e.g., inversion-dominated or not) of orogenic deformation. Furthermore, it is well known that the role of mechanical stratigraphy is extremely important as it impacts the style of deformation and the modes of strain localization. Price and Cosgrove (1990) provided a review of numerous analog models describing the behavior of deforming multilayers characterized by competence (i.e., viscosity) contrasts. These models show the coexistence of folding and faulting during the same deformation. In these multilayers, offering mechanical resistance to layer-parallel compression, folding occurs by buckling. Various studies pointed out the fundamental role played by mechanically dominant members in regional fold development as a result of buckling processes (Mazzoli et al., 2001; Morley, 1994), fold wavelengths being typically controlled by the thickness of such more competent "control units" (Cobbold, 1975; Price & Cosgrove, 1990). Widespread evidence of break thrusts that propagated across previously folded strata has been provided since the 1980s' (e.g., Cooper & Trayner, 1986; De Donatis & Mazzoli, 1994; Fischer et al., 1992; McNaught & Mitra, 1993). The importance of buckling as a viable mechanism for fold generation in thrust belts
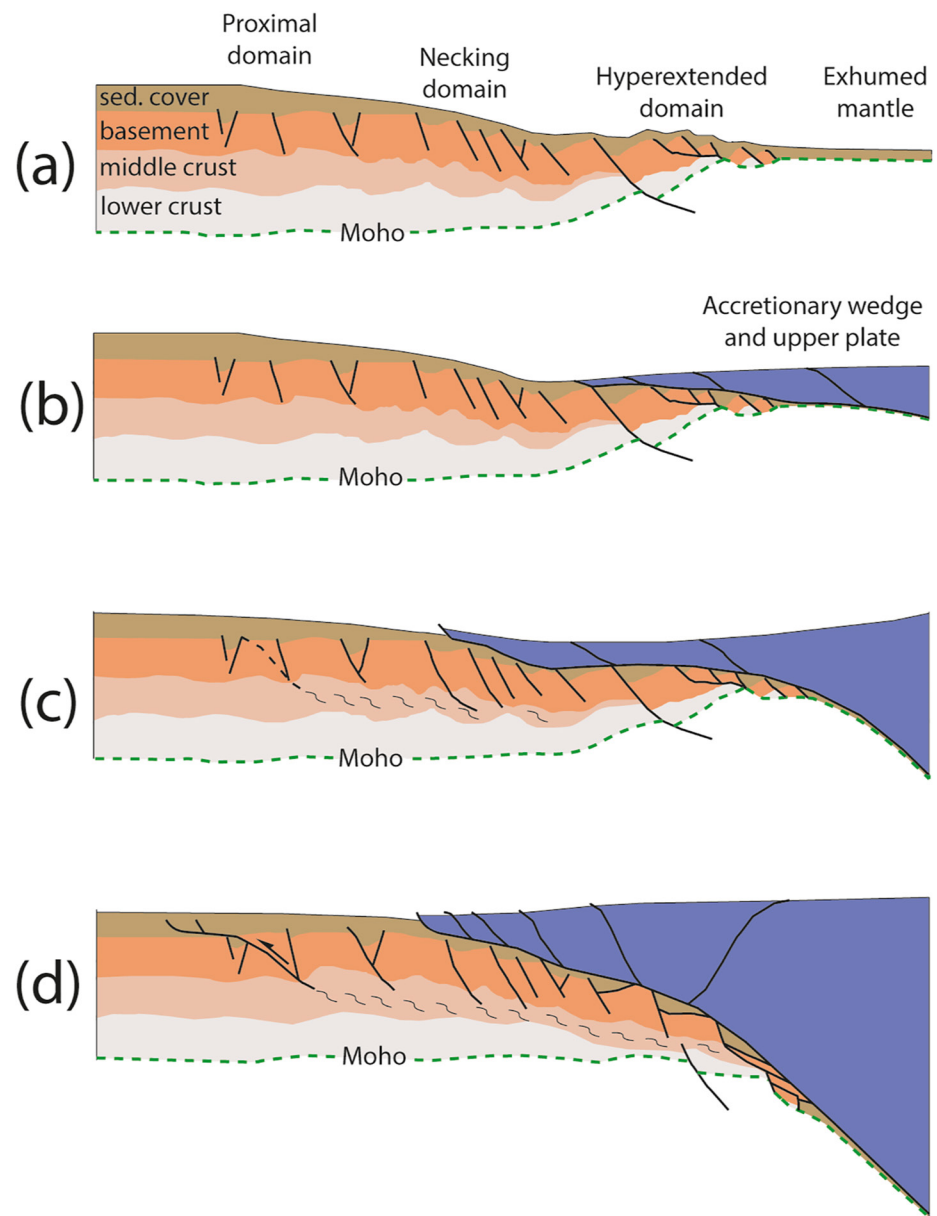
Figure 2. Cartoons showing the evolution of a rifted continental margin involved in continent-continent collision (after Tavani et al., 2021, modified). (a) Original setting of the rifted continental margin. (b) Continent-continent collision and propagation of a basal décollement within the deep-water succession of the hyperextend domain of the continental margin. (c) Involvement in the deformation of the shallow-water to slope succession of the necking domain of the continental margin. (d) Downward propagation of the deformation and reactivation of the middle crustal décollement of the necking and proximal domains of the continental margin. Development of basement thrust ramps in the frontal part of the fold and thrust belt.

was recently re-emphasized by Butler et al. (2019), who argued that most of the present-day structural interpretations are strongly focused on purely kinematic models (e.g., Jamison, 1987) that overlook the role of mechanically active layering. Very similar concepts were expressed already 30 years ago by Ramsay (1992), who was strongly critical towards the generalized acceptance and aprioristic application of similar geometric models—essentially involving forced folding in fault hanging walls—to all fold and thrust belts of our planet. After many years during which these concepts were largely ignored, the pivotal importance of understanding structural styles in fold and thrust belts is now becoming evident (e.g., Butler et al., 2018).

This paper focuses on the outer Albanides fold and thrust belt, where marked across- and along-strike changes in structural styles emerge from the analysis of published cross-sections (e.g., Bega & Soto, 2017; Durmishi et al., 2014; Frasheri et al., 2009; Robertson & Shallo, 2000; Roure & Sassi, 1995; Roure et al., 1995; Velaj, 2015b; Velaj et al., 1999). Such changes have never been organically discussed and explained, beyond generic invocations of the role of thickness variations of Triassic evaporites located at the base of the sedimentary cover. New balanced and restored geological sections across the southern outer Albanides are presented together with a strike section in order to provide a comprehensive picture of detachment-dominated thrusting of the sedimentary cover that largely characterizes this sector of the fold and thrust belt. As recent and active deformation of the entire frontal zone of the belt appear to be governed by ramp-dominated, basement-involved thrusting (Kamberis et al., 2022; Teloni et al., 2021; Vittori et al., 2021), our results also provide new insights into the development of mixed thrust tectonics styles (Figure 1b) that may result from space-time variations of both stratigraphic and rheological factors.

2. Geological Setting

Albania (Figure 3) includes an important segment of the Africa-vergent portion of the Mediterranean Alpine orogenic system, which in this part of Europe is constituted by the NW-SE striking Dinarides—Albanides—Hellenides mountain belt. This latter developed within the general framework of Africa-Eurasia major plate convergence, which involved (Kodra, Gjata, & Bakalli, 1993; Kodra, Vergely, et al., 1993; Vergely et al., 1998): (a) the subduction and eventual closure of a branch of the Tethys Ocean, (b) the Late Jurassic emplacement of ophiolitic units on top of the continental margin of Adria (or Apulia, a microplate originally forming part of Africa; Anderson & Jackson, 1987; van Hinsbergen et al., 2020), and (c) shortening of the continental margin of Adria. As it is common for mountain belts of the Alpine system, two major tectonic domains are defined also for the Albanides: the Internal—or inner—Albanides and the External—or outer—Albanides (e.g., Frasheri et al., 2009; Velaj, 2015b, and references therein). The tectonic units belonging to the two domains are briefly described below from the outermost to the inner ones, with the same order used in cross-section balancing and restoration.

The External (or outer) Albanides derive from deformation of a segment of the former Adria continental margin (e.g., Robertson & Shallo, 2000; and references therein). This included a series of shallow- and deep-water domains termed (from west to east): Sazani, Ionian, Kruja, and Krasta-Cukali zones. These domains formed by Triassic to Early Jurassic rifting (Roure & Sassi, 1995). Subsequently, they were included in the magma-poor, Adria rifted continental margin (Manatschal, 2004; Robertson & Shallo, 2000; Whitmarsh et al., 2001) that formed after the onset of seafloor spreading in the Tethys Ocean (Figure 4).

Subsequent shortening and top-to-the-WSW thrusting originated a series of tectonic units that conventionally maintain the names of the respective paleogeographic domains (e.g., Frasheri et al., 2009). The outermost Sazani units are exposed along the Adriatic coast of SW Albania. They are characterized by an Upper Triassic to Oligocene shallow-water carbonate succession representing the SE continuation of the Apulian carbonate platform exposed in Italy. The platform carbonates are overlain by a foreland basin succession of early Miocene—Pliocene age (Frasheri et al., 1996). The structurally overlying Ionian units consist of a series of thrust sheets derived from the Ionian basin, which was originally located between the Sazani (Apulian) carbonate platform to the west and a further carbonate platform (Kruja) to the east. The latter, interposed between the Ionian basin to the west and the ocean-continent transition to the east (Figure 4), can be regarded as an extensional ribbon like the Apennine platform of the southern Apennines (Mazzoli et al., 2014) or the Bisotun-Avalon platform of the Lurestan area of the Zagros Mountains (Vergés et al., 2011). The base of the Ionian basin stratigraphic succession, overlying an unknown basement generally assumed of crystalline—high grade metamorphic and/or igneous—nature (e.g., Kamberis et al., 2022), is formed by Permo-Triassic (Velaj, 2015b) to Upper Triassic (Burano Fm.) evaporites consisting of intercalated gypsum, anhydrides, dolomitic limestone, salt and varicolored shales and breccias (Velaj, 2001). It is worth noting that in the Apennines of central Italy, which involve a sedimentary succession pertaining to the same basin (Rubert et al., 2012; Zappaterra, 1994), deep wells penetrated Permo-Triassic siliciclastic deposits of the Verrucano Group (Anelli et al., 1994). Deep seismic reflection data (CROP 03) suggest that these Permo-Triassic deposits are locally several kilometers thick (Decandia et al., 1998). They are interpreted as the sedimentary fill of variably inverted half-grabens (Butler et al., 2004) originally associated with extensional/transtensional relaxation of the Variscan orogen (Bally et al., 1986). In the area of the present study,
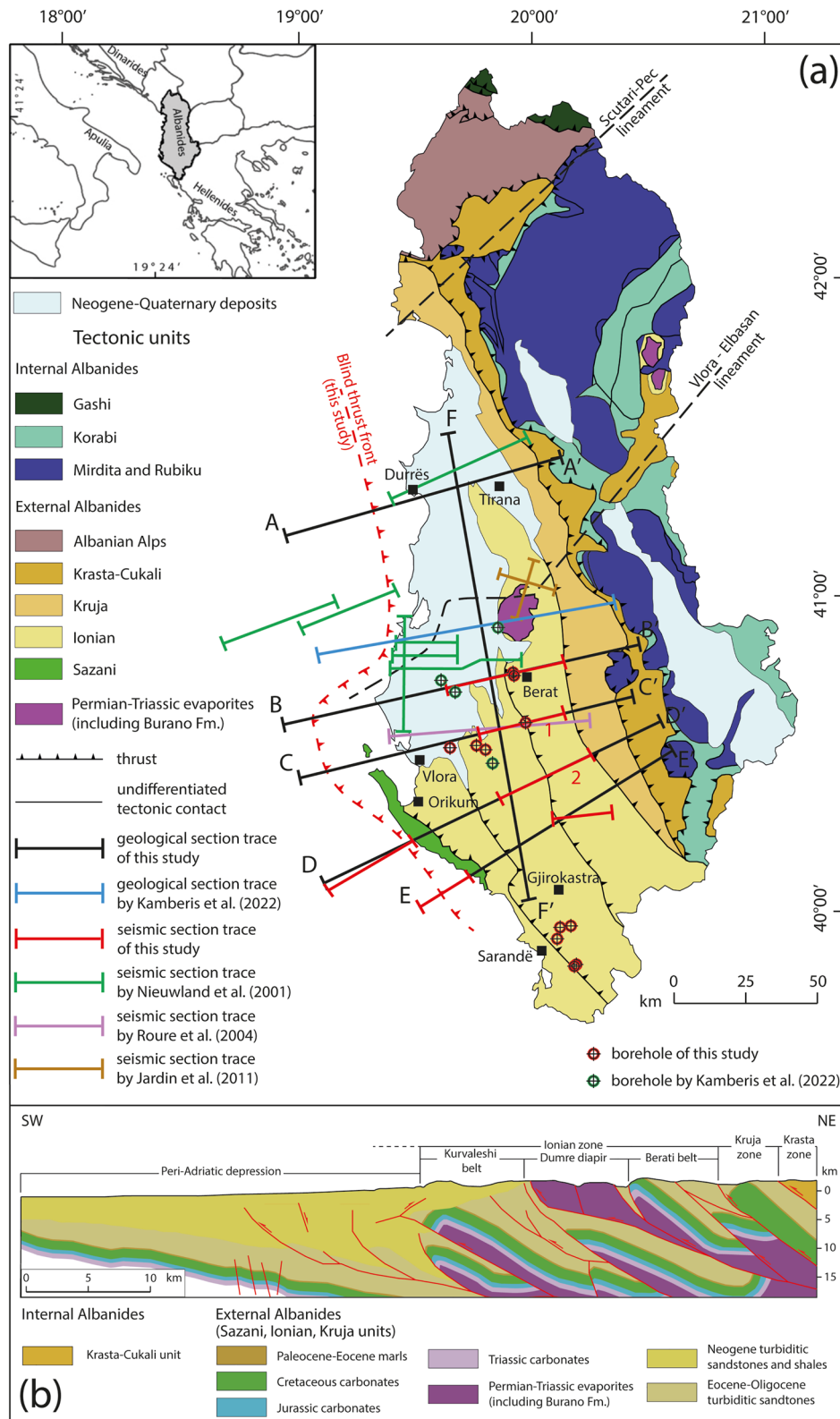
Figure 3. (a) Tectonic sketch map of Albania (modified after Muceku et al., 2008; Nieuwland et al., 2001; Roure et al., 2004; Teloni et al., 2021), showing traces of geological sections of this study and of seismic reflection profiles that aided their construction. Location of the seismic profiles published by Nieuwland et al. (2001), Roure et al. (2004) and Jardin et al. (2011) is also shown. (b) Geological section (after Kamberis et al., 2022, modified; the section is not balanced, as in original).
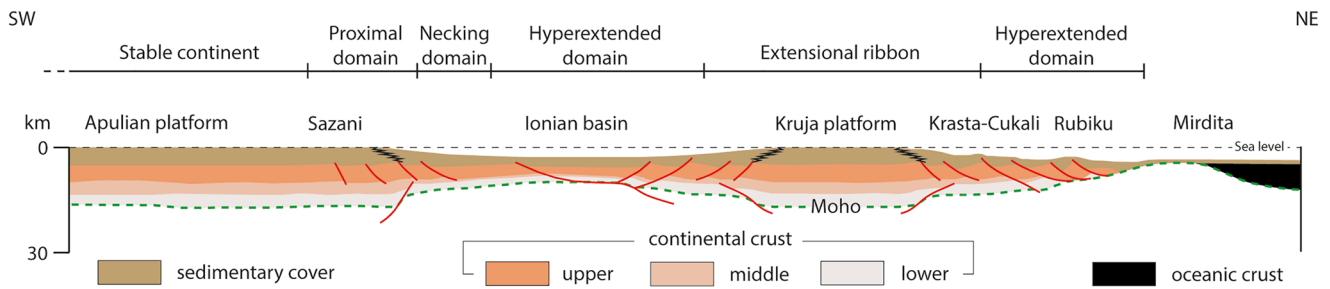
Figure 4. Schematic representation of the Early Jurassic setting of the Adria rifted continental margin in the study area.

Permo-Triassic deposits and the Burano Fm. are overlain by Upper Triassic (Norian-Rhaetian) dolomites, followed by Lower Jurassic successions that include both shallow-water and pelagic basin formations. These are followed upward by Mesozoic and Paleogene pelagic limestones, marls and shales (Mecaj & Mahmutaj, 1995; Zappaterra, 1990), and then by Oligocene sandstones, siltstones and marls recording turbiditic syn-tectonic sedimentation in a subsiding foreland basin (Bega & Soto, 2017; Roure et al., 2004). The tectonically overlying Kruja units consist of a Mesozoic-Paleogene carbonate platform succession topped by Oligocene syn-tectonic foreland basin sediments (Robertson & Shallo, 2000; Roure et al., 2004; Shehu, 1995). These units are overthrust by the Krasta-Cukali units, which consist of a sedimentary succession including Triassic volcanoclastic rocks and neritic limestones, Jurassic-Cretaceous deep-water clastic sediments, and Paleocene-Eocene pelagic limestones (Velaj et al., 1999). North of the Scutari-Pec "lineament" (discussed in the next section; Figure 3), the Albanian Alps constitute a distinct tectonic unit made of a Permian clastic succession overlain by Mesozoic platform carbonates and Paleocene-lower Eocene siliciclastic strata (Muceku et al., 2008).

The tectonically overlying Internal nappes were accreted to the Eurasian continental margin by the end of the Mesozoic (Velaj, 2015b). The Rubiku nappe is made of Triassic to Jurassic volcano-sedimentary strata (Muceku et al., 2006). The tectonically overlying Mirdita nappe consists of Middle Jurassic ophiolites including mantle units (Bortolotti et al., 1996; Saccani et al., 2017). The topmost Korabi nappe includes a low-grade metamorphic basement (ascribed to the Paleozoic), which is overlain by Permo-Triassic siliciclastic rocks and a carbonate platform succession of Triassic to Jurassic age (Tremblay et al., 2015). This nappe is thought to have originated from a continental block originally located east of the Mirdita oceanic domain (e.g., Robertson & Shallo, 2000), although a different paleogeographic location has also been proposed (e.g., Vilasi, 2009; Vilasi et al., 2009, and references therein). North of the Scutari-Pec "line", the Internal Albanides include the Gashi nappe, which consists of Permian-Triassic metamorphic rocks and overlying carbonates (Prenjasi et al., 2011).

2.1. Tectono-Sedimentary Framework of the Outer Albanides

A major flexural basin developed on top of the foreland lithosphere during the late Oligocene as a result of the tectonic load provided by the orogenic edifice, which at the time was formed by the large-displacement Krasta-Cukali units and the structurally overlying inner Albanides nappes (including the Mirdita ophiolite). The fold and thrust belt includes different structural provinces roughly bounded by transversal tectonic "lineaments" such as the Scutari-Pec and the major, NE-trending Vlora-Elbasan ones (Figure 3). These transversal structural features are commonly interpreted as major Cenozoic transfer zones of the thrust belt (e.g., Durmishi et al., 2014). For the Vlora-Elbasan zone in particular, a control by an inherited deep-seated basement fault has been inferred (e.g., Lacombe et al., 2009). Nieuwland et al. (2001) interpreted this structure as a Triassic/Jurassic strike-slip fault.

The structural province located southeast of the Vlora-Elbasan "lineament" is characterized by extensive outcrop of folded and imbricated Meso-Cenozoic sedimentary successions of the Ionian basin, detached along Triassic evaporites. These latter form large, NNW striking diapiric walls observed in seismic lines (Kamberis et al., 2022; Roure et al., 2004; Velaj, 2015b). Significant halokinesis of the Triassic evaporites is also evidenced by numerous, variable sized diapirs that reached the surface (e.g., Bega & Soto, 2017; Jardin et al., 2011; Robertson & Shallo, 2000; Velaj, 2001, 2015b). The largest of them is the Dumre diapir, which is clearly involved in thrust-related deformation (Figure 3b). Besides the diapirs, the structural architecture is dominated by faulted and

WSW-transported, often doubly verging anticlines (Kamberis et al., 2022, and references therein). The analysis of syn-tectonic growth strata indicates that deformation of the Ionian basin progressed forelandward, starting in late Oligocene-Aquitanian times to the east and continuing during Langhian–Serravallian times more to the west (Lacombe et al., 2009). This deformation led to the development of three main antiformal ridges (termed Berati, Kurvaleshi and Cika belts; Figure 5) largely transported southwestward by major thrusts rooting into the Triassic evaporites (Nieuwland et al., 2001). The Berati and Kurvaleshi belts consist of regional anticlinoria including in their interior a series of anticlines and synclines. These anticlinoria are cored by Triassic evaporites, which attain a very large (multi-kilometric) thickness beneath the Berati belt (Velaj, 2011, 2015b; and reference therein). The Cika belt is a smaller anticlinal relief located close to the tectonic boundary with the outcropping Sazani carbonate platform domain (Durmishi et al., 2014). These antiformal belts were the focus of extensive studies, due to the presence of important petroleum systems (e.g., Curi, 1993; Diamanti et al., 1995; Durmishi et al., 2014; Frasheri et al., 2009; Velaj, 2015b; Velaj et al., 1999). Recently, the interest for suitable reservoir rocks involved in structural traps within the Ionian zone (both onshore and offshore in the Adriatic Sea) has become increasingly important because they are considered excellent targets for gas/energy storage (Hatziyannis et al., 2009; Proietti et al., 2021) as part of the ongoing energy transition process.

The structural province located northwest of Vlora-Elbasan "lineament" is characterized by a flexural foreland basin hosting an up to 10 km thick siliciclastic succession of Oligocene to Quaternary age. This deep foreland basin, known as Peri-Adriatic Depression, includes shallow-water deposits in its eastern and southern portions, and deeper water (mainly turbiditic) sediments in the northern and western (offshore) sectors (Lacombe et al., 2009; and references therein). In this northern structural province, available seismic lines show no major basement-cover decoupling along the Triassic evaporites, and the Ionian basin succession is interpreted as essentially attached to the basement (Roure et al., 2004; Santini et al., 2020; Teloni et al., 2021). The overlying Cenozoic foredeep succession is deformed by thrust imbrication and minor duplexing in the eastern part of the Peri-Adriatic Depression (Roure et al., 2004). The latest stages of this deformation appear to reach early Pliocene times, based on the constraints provided by syn-tectonic deposits (Nieuwland et al., 2001; Roure et al., 2004). On the other hand, the most recent deformation occurred forelandward, along an active basement ramp forming the blind thrust front beneath the western portion of the Peri-Adriatic Depression (Teloni et al., 2021).

3. Balanced Cross-Section Construction and Restoration

Four balanced sections were constructed across the study area of the southern outer Albanides, where unpublished subsurface data (seismic lines and deep well logs) were made available to us (Figure 5). In this study area deformation was substantially controlled by the occurrence of an efficient décollement layer—represented by the Triassic evaporites—at the base of the Ionian Basin succession. As our study is focused on the outer-frontal portion of the fold and thrust belt, balancing and restoration was carried out for the tectonic units (Sazani, Ionian, and part of the Kruja) located in the footwall of the Krasta-Cukali units. The balanced cross-sections were restored using common deformation algorithms incorporated into Move software (Petroleum Experts).

To highlight the along-strike change in structural style, a geological section across the northern outer Albanides (trace A-A′ in Figure 3) by Teloni et al. (2021) was also revised, balanced and restored using Move software (Petroleum Experts). Recent seismological data provided pivotal information on basement involvement in thrusting along this section. The 2019–2020 Durrës seismic sequence was in fact characterized by an eastward deepening hypocenter distribution ranging in depth from 10 to 36 km (source: https://earthquake.usgs.gov/earthquakes/search/ and http://rcmt2.bo.ingv.it/; last access: 24 January 2022). The M_w = 6.4 main shock (located at a depth of 22 ± 1 km) and most of the earthquakes of this sequence were nucleated along a major NNW striking basement thrust ramp defining the blind thrust front in the northern outer Albanides (Teloni et al., 2021; Vittori et al., 2021). Finally, a strike section was constructed along trace F-F′ in Figure 3 from the northern to the southern outer Albanides and across the Vlora-Elbasan "lineament".

Building of the geological sections across the southern outer Albanides was based on published geological maps (Viti, 2014; Xhomo et al., 2002) integrated with our own field observations, available stratigraphic information and seismic interpretation, both calibrated with deep well logs. Bedding data from a 10 km wide domain surrounding the onshore segment of each dip cross-section trace indicate sub-cylindrical folding (Ramsay & Huber, 1987) around a sub-horizontal statistical axis. The thrust belt curvature observable from the geological
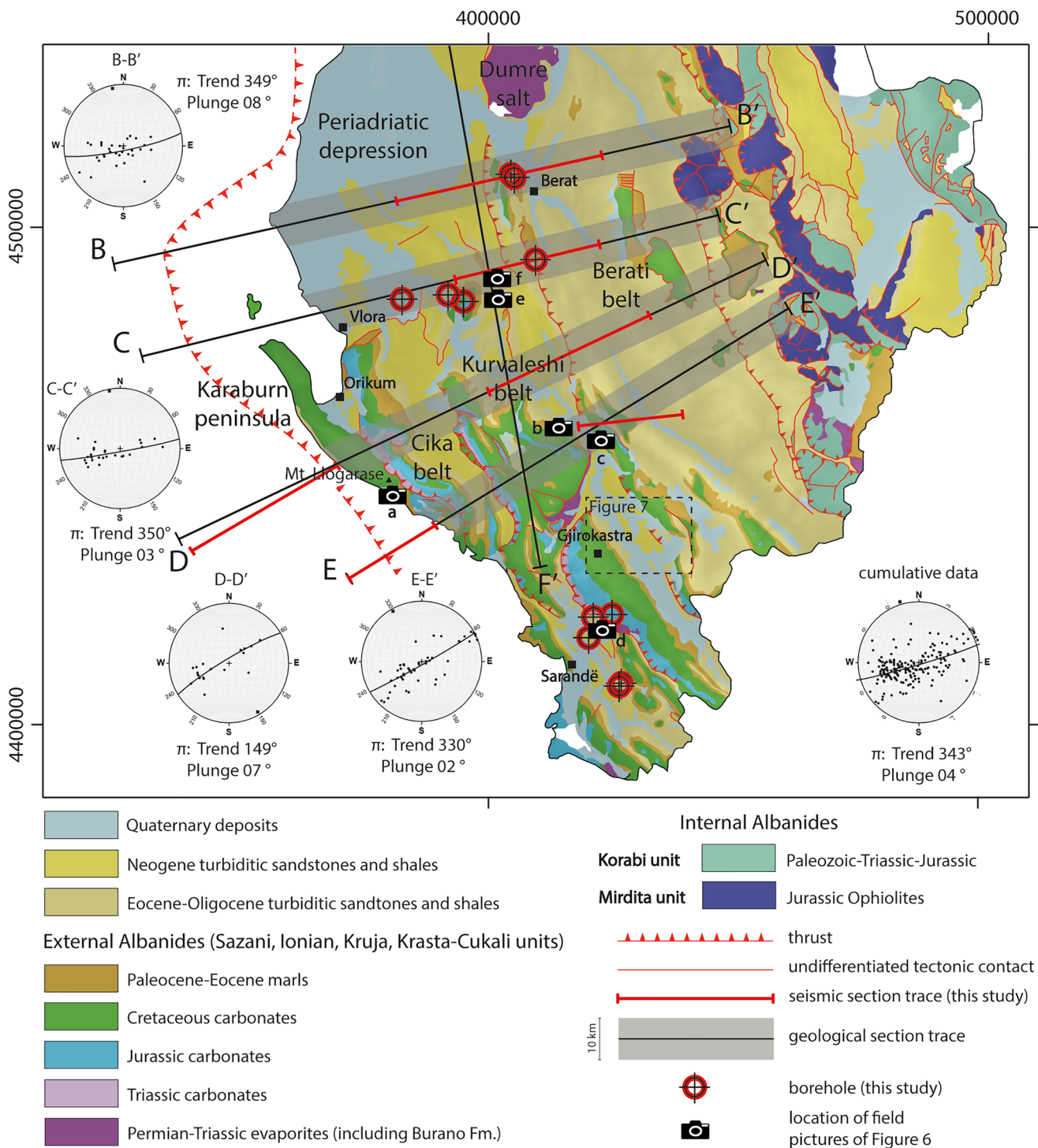
Figure 5. Geological map of southern Albania (modified after Muceku et al., 2008; Roure et al., 2004; Teloni et al., 2021; Xhomo et al., 2002) draped onto a digital elevation model (source: https://www.eea.europa.eu/; last access: 24 January 2022), showing location of deep wells and seismic profiles, and of the cross-sections produced in this study (trace of strike section F-F′ continuing northward is shown in Figure 3). Bedding attitude data are plotted on lower hemisphere, equal area projections (poles to bedding are shown together with the best-fit great circle approximating their distribution and the related pole, which provides the π statistical fold axis). Plots related with individual cross-sections include data collected from the 10 km wide gray boxes surrounding each cross-section trace. The location of the field pictures of Figure 6 and of the map of Figure 7 are also shown.

map of the southern outer Albanides is consistently accompanied by a southward change of fold axes orientation from a NNW to a NW trend (Figure 5). This results in a larger scattering of bedding data in the cumulative plot, which anyway still shows sub-cylindrical folding around a sub-horizontal, NNW trending statistical axis (Figure 5). Major folds display wavelengths ranging from several kilometers, for the regional anticline involving the Sazani platform carbonates exposed in the Karaburn peninsula-Mt. Llogarase region (Figure 6a), to few kilometers and down to the hundreds of meters for the folds involving the Ionian Basin succession (Figure 6b). In the latter, minor folds of tens to a few meters' wavelengths (Figure 6c) occur as parasitic folds associated with the major structures. The largely dominant calcareous strata of the Ionian Basin succession show a spaced, disjunctive pressure-solution cleavage generally perpendicular or at very high angle to bedding (Figure 6d). Striae and calcite shear fibers often observed on bedding surfaces are roughly normal to the bedding-cleavage intersection lineation (Figure 6e), which in turn is generally parallel to fold hinges, indicating bedding-parallel slip during flexural-slip folding. A discontinuity network (whose analysis is beyond the scope of this regional study) constituted by joints and bedding planes allowed for significant fluid flow, as testified by bitumen impregnations locally observed in Cretaceous-Paleogene limestones of the Ionian Basin succession (Figure 6f).

The reported field evidence provides information on the dominant folding mechanism in the study area. Parasitic folds are a result of polyharmonic folding, a process controlled by competence contrasts among beds of different viscosity within the framework of mechanically active layering at various scales (Ramsay & Huber, 1987). Similarly, the development of cleavage at a high angle to bedding, resulting in convergent cleavage fans in folds, is a record of tangential longitudinal strain in competent layers and of limited or no modification of the early cleavage produced by initial layer-parallel shortening preceding fold amplification in mechanically active multilayers (Ramsay, 1967). Cleavage patterns (i.e., finite strain trajectories) and layer thickness variations in beds of differing competence are all indicative of buckle folding (Ramsay, 1981). Outcrop-scale features are consistent with map-scale structures, which are commonly characterized by folds/fold trains occurring in both hanging wall and footwall blocks of thrust faults. Single folds showing abrupt plunge terminations (Figure 7) form part of fold arrays typically associated with buckling (Price & Cosgrove, 1990, and references therein). It is worth noting that almost all published detailed geological sections across the outer southern Albanides show variably offset and/or truncated folds, with the common occurrence of faulted fold trains, well-developed footwall synclines, and reverse faults cutting across the intermediate limbs of antiform-synform pairs (e.g., Durmishi et al., 2014; Kamberis et al., 2022; Frasheri et al., 2009; Velaj, 2001, 2011,; Velaj et al., 1999; Figure 3b). These features indicate that in most cases folds were not generated passively (i.e., as forced folds; Butler et al., 2019) by the motion of rock panels above stepped thrust as postulated in fault-related folding models (e.g., Jamison, 1987). Rather, most folds were modified by thrusts and/or developed coevally with thrusts as distinct types of mechanical instabilities. Early buckle/detachment folds—Butler et al. (2019) demonstrated that there is no real difference between these two fold types—are clearly offset, modified and largely displaced by thrust faults detaching along Triassic evaporites (e.g., Nieuwland et al., 2001).

3.1. Stratigraphic Constraints

As the balanced and restored geological sections across the southern outer Albanides (located in Figure 5) involve the sedimentary successions of the Sazani, Ionian and (partly) Kruja zones, a composite template was built including the stratigraphy of the three zones (Figure 8). Such a stratigraphic template was obtained by integrating published information and surface geological data with the constraints derived from the analysis of deep well logs (whose projected position is shown in Figure 8). Depth-converted reflection seismic profiles, calibrated using the same well logs, were also used in the process. The resulting multilayer includes: (a) a pre-Triassic crystalline basement; (b) a variable thickness of Triassic evaporites (forming the main décollement level for the fold and thrust belt); (c) an Upper Triassic to Eocene, carbonate passive margin succession; and (d) an Eocene to Pliocene (to Quaternary offshore), syn-tectonic turbiditic succession, discontinuously overlain by Quaternary continental deposits onshore.

Overlying Triassic evaporites, the Sazani carbonate platform is shown in the template with a thickness of 2,380 m of Triassic and 555 m of Jurassic dolomites. These are overlain by a total of 1,270 m of Cretaceous-Paleogene shallow-marine limestones and dolomitic limestones, for a cumulative thickness of 4,205 m. Eastward, a facies change (east-dipping paleoslope) marks the transition between the Sazani carbonate platform and the Ionian basin. This latter was a fault-controlled extensional basin in which large volumes of evaporites were deposited.
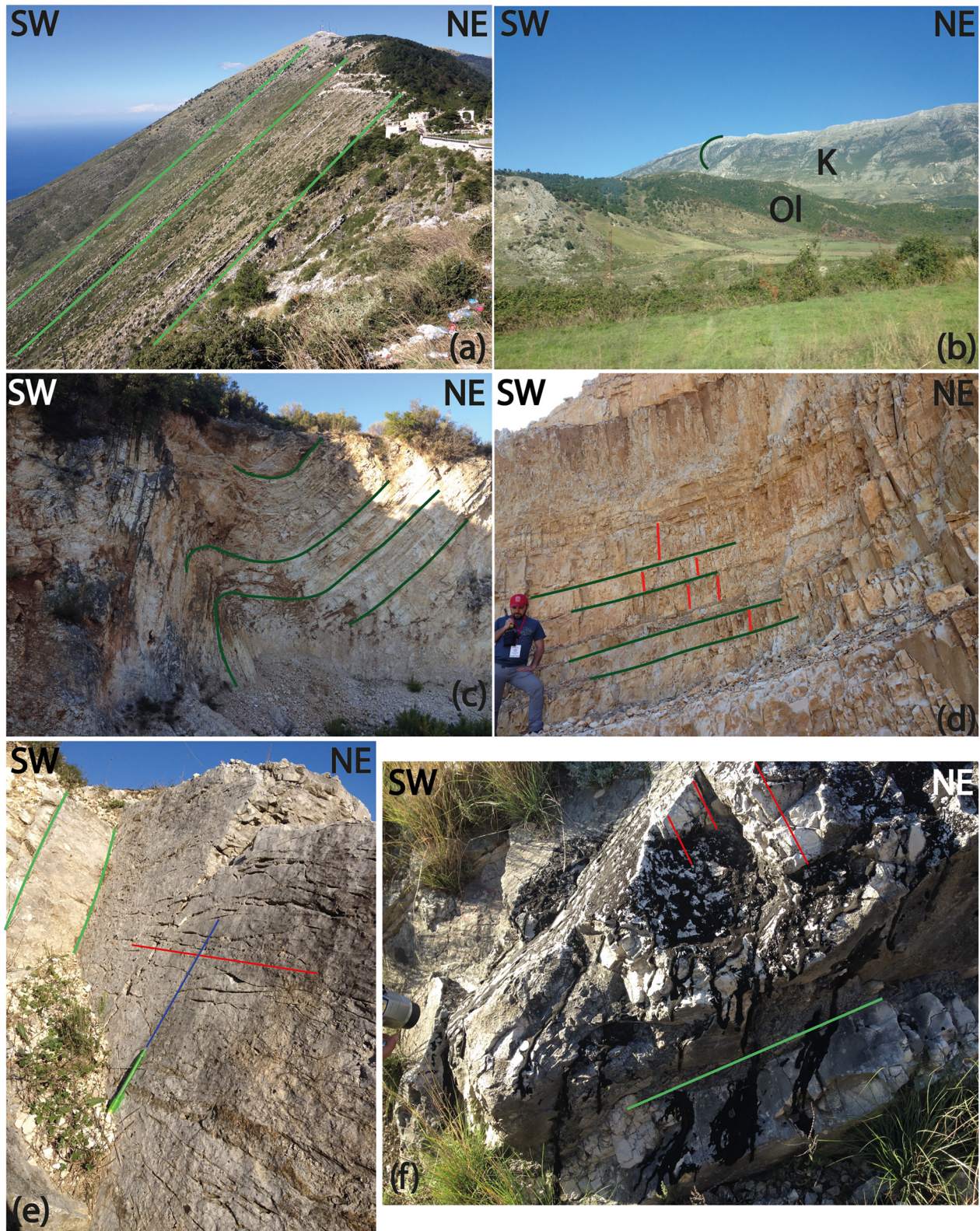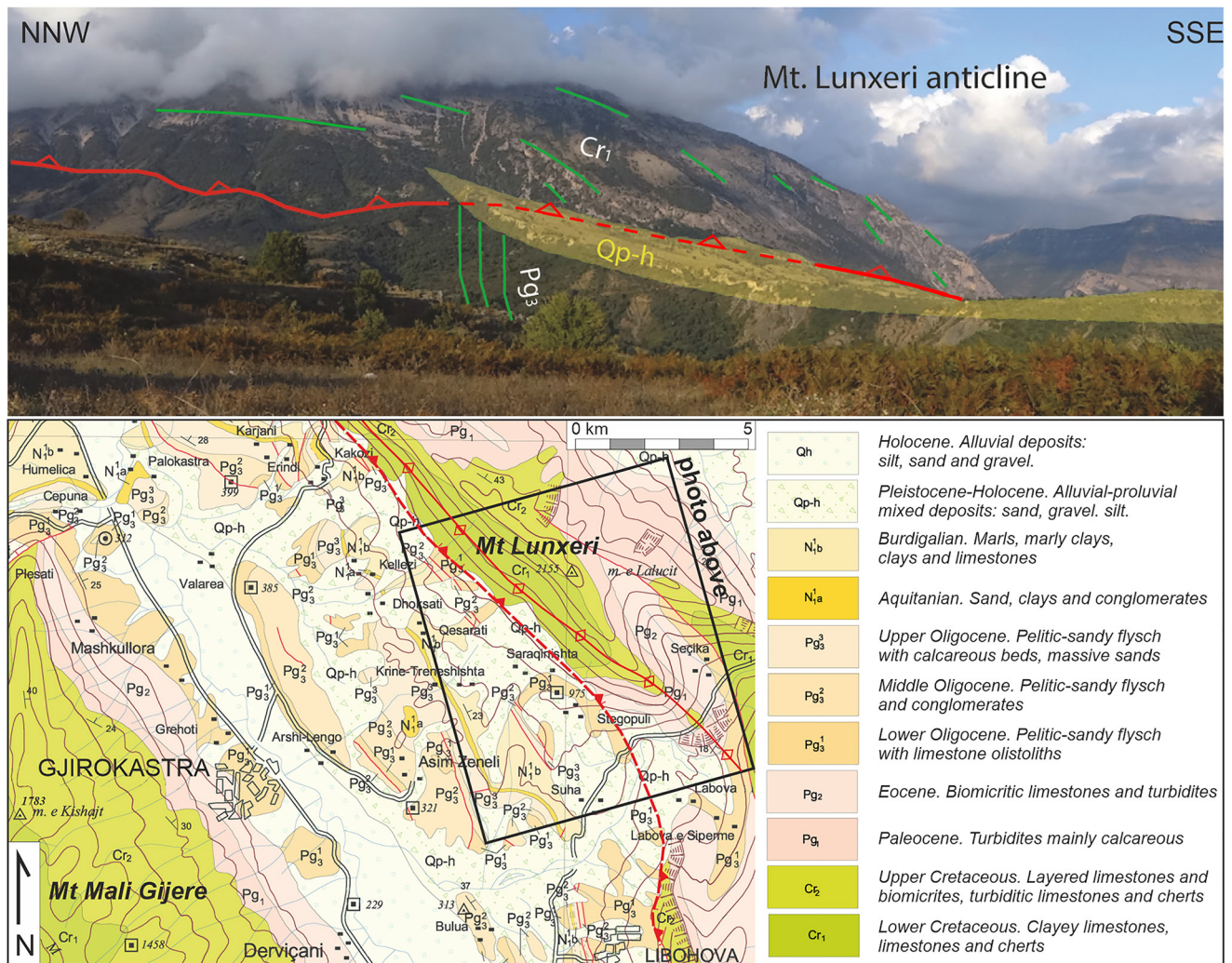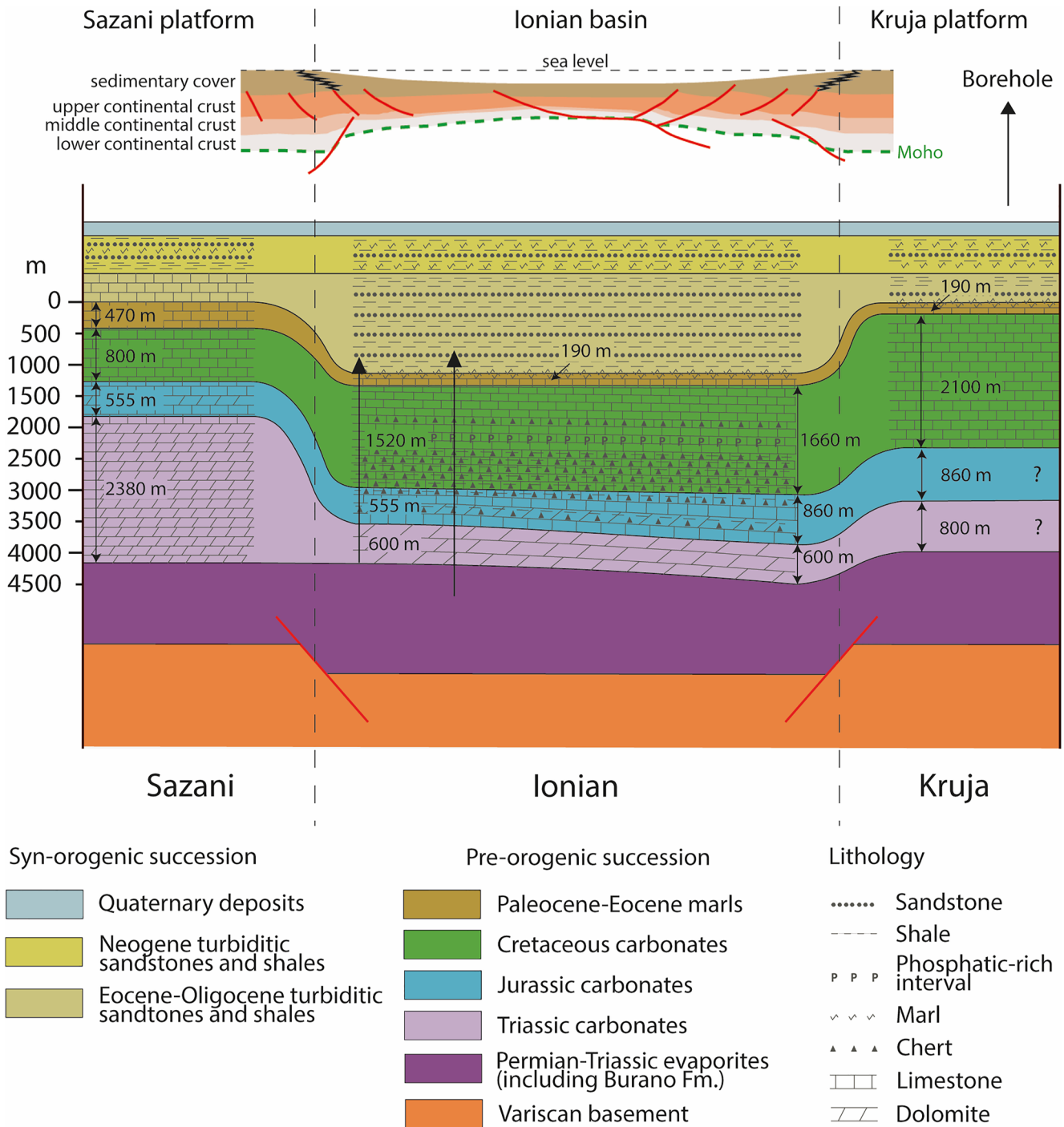
Figure 6.

Figure 7. Geological map (located in Figure 5; modified after Viti, 2014) and view of the SE-plunging periclinal termination of the Mt. Lunxeri anticline (Berati belt) in the hanging wall of the thrust separating Cretaceous carbonates (Cr1) from vertical Oligocene beds (Pg3) in the footwall (Kurvaleshi belt).

The overlying Upper Triassic to Eocene pelagic succession is characterized by a generally eastward increasing thickness (Velaj et al., 1999). In our stratigraphic template, the total thickness of the Ionian basin succession is shown to range from 2,865 m to the west to 3,310 m to the east (minor local variations, which are likely to characterize the syn-rift lower part of the Mesozoic succession, are not shown as they could not be identified along our geological transects). Farther eastward, the transition between the Ionian basin and the Kruja carbonate platform is marked by a west-dipping paleoslope. The Kruja platform is characterized by a thick Cretaceous succession (2,100 m in our stratigraphic template; Roure et al., 2004) overlain by Paleogene carbonates (190 m). The Triassic-Jurassic part of the platform succession is unknown as the Kruja units are detached along Lower Cretaceous evaporites (Roure et al., 2004). The indicative thickness shown in our template for the Triassic-Jurassic portion of the Kruja platform is anyway irrelevant within the framework of this study, as this part of the succession is not included in our geological sections (and is shown only schematically in the restorations).

Figure 6. Field pictures (located in Figure 5; bedding is traced in green for all diagrams). (a) Southwest dipping strata in the forelimb of the regional anticline involving shallow water Cretaceous-Paleogene carbonates of the Sazani units at Mt. Llogarase. (b) Overturned anticline involving the Ionian Basin succession of the Berati Belt (Cretaceous limestones forming the background relief, K; hanging-wall block) overthrusting Oligocene foreland basin deposits of the Kurvaleshi Belt (in the foreground, Ol; footwall block). (c) Minor folds in Cretaceous limestones of the Ionian Basin succession exposed in the Berati Belt. (d) Spaced, disjunctive pressure-solution cleavage in Cretaceous limestones of the Ionian Basin succession exposed in the Berati Belt. (e) Detail of bedding surface in Cretaceous limestones of the Ionian Basin succession exposed in the Kurvaleshi Belt, showing flexural-slip-related striae and calcite shear fibers (blue) perpendicular to the bedding-cleavage intersection lineation (red). (f) Same lithology as in (e), impregnated by bitumen (cleavage surfaces are shown in red).

Figure 8. Integrated stratigraphic template for the Sazani, Ionian and Kruja zones of the southern outer Albanides. Projected location of deep well logs used for integrating the calibration is shown. The Triassic-Jurassic section of the Kruja zone is indicative, as this part of the succession is unknown (see text).

The Eocene to Pliocene turbiditic sandstones and shales, not considered in our restorations, are shown schematically in the stratigraphic template (with an approximate thickness) as an upper layer across the Sazani, Ionian and Kruja zones. The succession is topped by Quaternary deposits (schematically depicted as a continuous layer in the template but strongly heterogeneous, particularly for onshore continental sediments).

3.2. Seismic Interpretation

The interpretation of seismic reflection profiles made available to us, calibrated with exploration well logs, significantly helped constraining our cross-sections (Figure 9). The seismic signal is generally coherent, allowing the interpretation of deep structures. The lithological change between the top of the carbonate succession and the stratigraphically overlying Eocene-Oligocene turbiditic sandstones and shales is marked by a strong acoustic impedance contrast. This, in turn, produces a strong reflection that effectively guides the interpretation (Figure 9). Focusing the seismic interpretation on this reflector, it is possible to interpret folds and thrusts, and to follow in the subsurface the structures observed at the surface.

In the seismic profiles, the reflectors within the syn-tectonic strata are characterized by condensation towards the crests of the anticlines, associated with convergent onlap on the fold limbs (particularly well observed in the forelimb of the regional faulted anticline involving the Sazani units in the coastal area and adjacent offshore). These features testify the syn-deformation nature of the Eocene-Oligocene turbiditic sandstones and shales, which were clearly deposited during coeval fold growth. Consistently with field observations, interpreted structures include dominantly SW verging folds, NE dipping thrusts and subordinate SW dipping backthrusts. The carbonate thrust sheets are underlain by Triassic evaporites, which provide the décollement. These display more chaotic seismic facies and vary in thickness, generally thinning in the direction of thrusting, as also observed in seismic profiles north of our study area by Nieuwland et al. (2001). A large amount of Triassic evaporites is interpreted, especially in the core of the larger anticlines, overlying the basement. The latter is also interpreted as locally faulted and involved in deformation, although a top basement reflector is only discontinuously picked in the seismic lines.

3.3. Restoration Algorithms

Sequential restoration is a widely applied procedure to check the geometric viability of geological structures. It is used to validate seismic interpretation and in cross-section balancing, and to reconstruct tectonic scenarios (e.g., Castelluccio et al., 2016; Tavani, Parente, Puzone, et al., 2018; Verwater et al., 2021). In this work we used the flexural-slip algorithm to restore the folds and the move-on-fault algorithm to restore the faults. The application of the move-on-fault tool, in turn, involved Fault Parallel Flow and Trishear for the thrusts, while Simple Shear was used for the normal faults.

The Fault Parallel Flow algorithm (Egan et al., 1999; Kane et al., 1997) is based on the principle of Particulate Laminar Flow over a fault ramp. It allows to: (a) preserve the forelimb area; (b) keep the footwall undeformed and not translated; and (c) preserve the line-length of horizons in parallel systems.

The Trishear algorithm (Erslev, 1991) is designed to model geological structures in 2D by deforming areas within a triangular zone of shear emanating from the tip of a propagation fault. The shape and location of the shear zone can be defined by tuning various geometrical parameters. Area preservation is maintained within the trishear zone during deformation, while outside it the hanging wall is deformed by Fault Parallel Flow.

The Simple Shear algorithm (Gibbs, 1983; Verrall, 1981; Withjack & Peterson, 1993) is used to model penetrative deformation that occurs throughout the hanging wall rather than discrete slip between bedding planes. It permits to control the restoration through the distance of movement and the shear vector, considering the theoretical gap created by extension between the fault plane and the hanging-wall block; therefore, the area of the hanging wall is preserved and the length between the fault plane and a marker horizon in the hanging wall is maintained.

3.4. Sequential Restoration and Basement Forward Modeling

Seismic interpretation calibrated by deep well logs and surface geological constraints were integrated in the construction of balanced geological sections. For each section, the Triassic to Eocene carbonate succession was divided into a series of fault-bounded blocks. Each block was unfolded using the flexural-slip algorithm taking into account the southwestward propagation of deformation clearly recorded by syn-tectonic deposits (e.g., Durmishi et al., 2014). Each fault was then restored to annul the displacement and to match the blocks. As it is common practice during a sequential restoration procedure, the fault traces shown in the restored sections consist of smoothed polylines that were constructed by linking the restored cut-off points avoiding zigzag effects (Santini
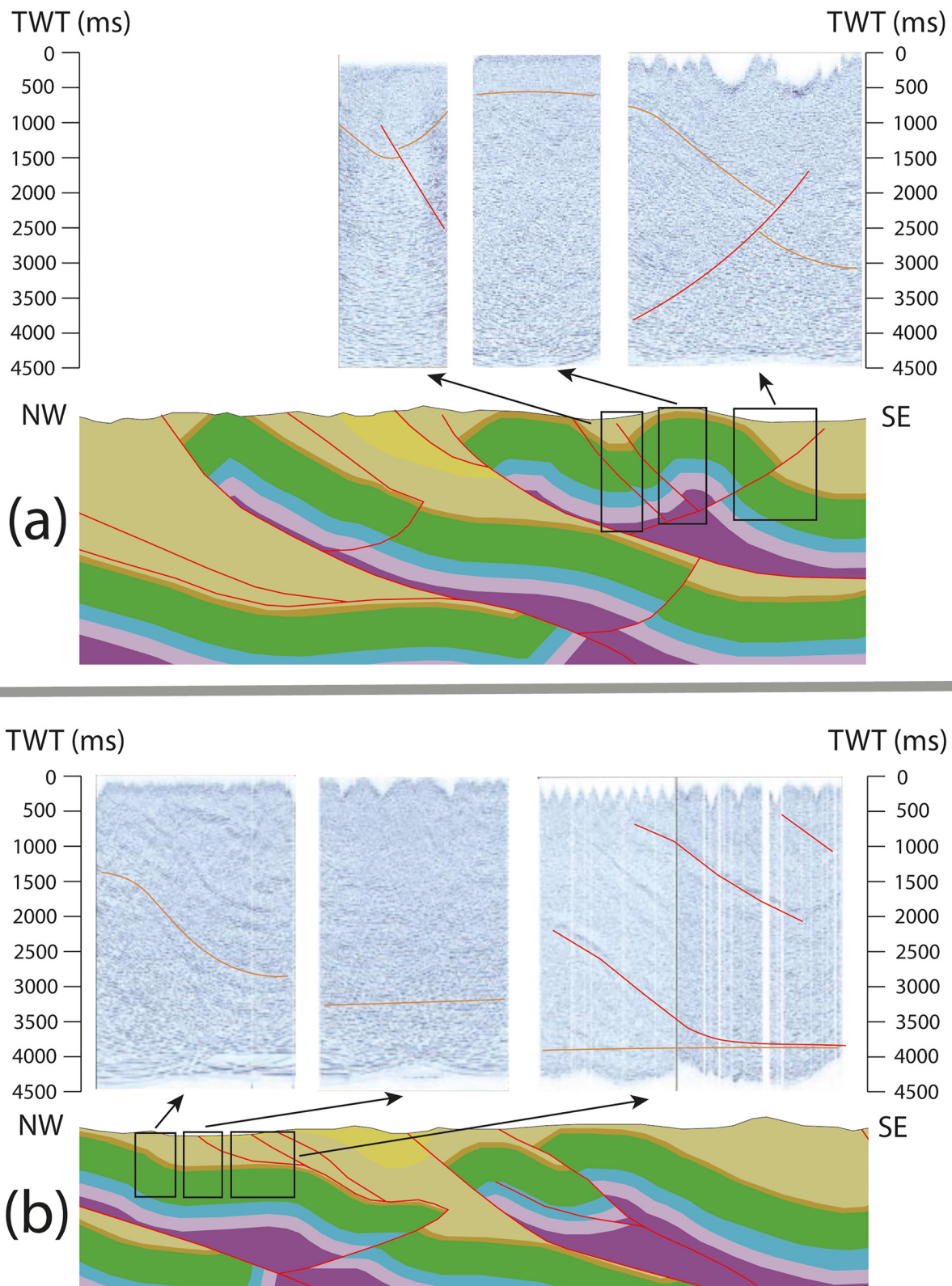
Figure 9. Examples of geological sections constructed along seismic reflection profiles (located in Figure 3). Lower-quality, small parts (previously published by Nieuwland et al., 2001) of the seismic profiles used in this study are shown above each of the sections, which however were constructed using the confidential seismic profiles. The top-carbonate reflector (see text) is marked. (a) Section (belonging to regional section C-C′ located in Figure 5) based on seismic interpretation of profile 1. (b) Section (belonging to regional section D-D′ located in Figure 5) based on seismic interpretation of profile 2.

et al., 2020; Tavani, Parente, Puzone, et al., 2018). Anyway, such a final smoothing never exceeded 0.5% of the original cut-off point position.

The sequentially restored carbonate succession was then used as a starting template for the reconstruction of the underlying Variscan basement, whose top was constrained integrating discontinuous seismic evidence with restoration preserving the area occupied by Triassic evaporites along the section. Although this type of restoration may be unsuitable to validate small-scale details of interpretations in areas of important salt-related deformation, Rowan and Ratliff (2012) pointed out it is certainly valuable in larger-scale interpretations such as those of this study. 2-D forward modeling involving the basement was subsequently performed for each section, until the final deformed state was reached. Forward modeling was not performed for the sedimentary cover, whose sequentially restored stages were coupled with basement forward modeling. This latter must be coherent with the balanced geological section built in the previous step, thereby providing a further validation of the structural interpretation. The basement was deformed using Simple Shear, Fault Parallel Flow and Trishear algorithms, which provided the best match with the available—though discontinuous—top basement geometry obtained from seismic interpretation.

4. Results

Balanced and restored sections are shown in Figures 10 and 11, together with a strike section in Figure 11. Section A-A′ across the northern outer Albanides shows a ramp-dominated, basement-involved deformation style (Figure 1a) in the Sazani and Ionian units, consistent with previous work by Roure et al. (2004), Santini et al. (2020) and Teloni et al. (2021). According to these authors, here the evaporites did not act as a décollement level, most probably due to their limited thickness. On the other hand, the Kruja units, detached along Lower Cretaceous evaporites, are relatively far traveled along this section. They form an imbricate fan sealed by a pre-Messinian unconformity (Lacombe et al., 2009; Roure et al., 2004). This results in the easternmost portion of the section being characterized by a mixed deformation style involving ramp-dominated thrusting in the basement and detachment-dominated thrusting in the sedimentary cover, associated with the Kruja thrust. A series of thrusts splaying out from the latter also deform Cenozoic foredeep strata of the Periadriatic Depression, forming a triangle zone of intercutaneous wedge type (McClay, 1992). The backthrust at the top of the intercutaneous wedge offsets the pre-Messinian unconformity, indicating that youngest thrust activity reached the early Pliocene (Nieuwland et al., 2001; Roure et al., 2004). Part of the thrust slip is also shown in section A-A′ to be passed to a pop-up involving the Neogene clastic succession (penetrated by a hydrocarbon exploration well; Santini et al., 2020) farther west. In the footwall of the Kruja thrust, a relatively low-displacement, basement-rooted reverse fault offsets the Mesozoic platform-to-basin transition (Kruja paleoslope) based on seismic interpretation by Roure et al. (2004). The latter interpretation also links the shallow pop-up located further west with a steep backthrust that is probably rooted down into the basement. The thrust front, which is marked by a hanging-wall anticline imaged by offshore geophysical data (Frasheri et al., 2009), is defined by a blind fault. This consists of a moderately to gently dipping—at the hypocentral depth of the M_w 6.4, November 2019 earthquake—basement thrust. Total horizontal shortening of the sedimentary cover along this section, measured using a pin line located in the immediate footwall of the frontal thrust ramp (for uniformity with respect to the southern sections), amounts to 43 km. Considering the restored length of the sedimentary cover for the same tract amounts to 111 km, the shortening is 38%. This is mainly associated with the Kruja thrust (accounting for 42 km of shortening), as the basement and the overlying—attached—Ionian succession show rather limited shortening (Table 1). West of the blind thrust front along this section, a few extensional faults are imaged by seismic data in the outer edge of the flexural foreland basin and in the Sazani (Apulia) carbonate platform involved in the fore-bulge (Frasheri et al., 2009). These normal faults, included in section A-A′, are best related to the well-known processes of outer-arc extension affecting the outermost sector of the foredeep and the peripheral bulge and in response to lithospheric bending associated with foreland flexuring (e.g., Doglioni, 1995; Tavani, Parente, Vitale, et al., 2018; Turcotte & Schubert, 2014). Some of these structures could also have developed by the reactivation of inherited, Mesozoic rift-related extensional faults (Teloni et al., 2021).

A mixed deformation style involving ramp-dominated thrusting in the basement and detachment-dominated thrusting in the sedimentary cover characterizes the sections across the southern outer Albanides (B-B′, C-C′, D-D′ and E-E′). Here, thick Triassic evaporites occur beneath the carbonate Ionian basin succession, thus providing an efficient décollement throughout most of the thrust system. A meaningful comparison of the amounts
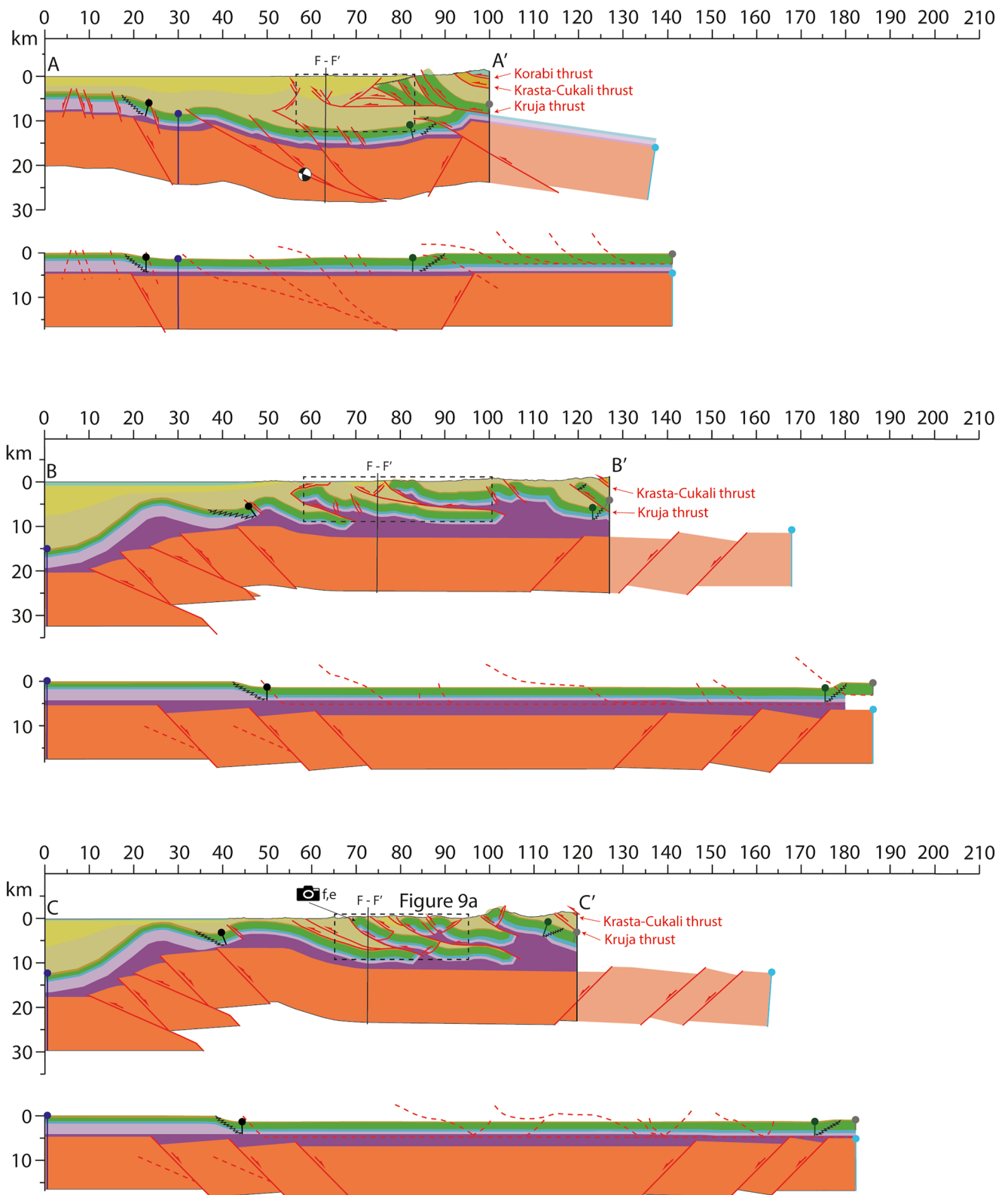
Figure 10.

of shortening can be carried out by taking into account structurally equivalent segments of each cross-section using the measured values provided in Table 1. Referring to measurements carried out using a pin line located in the immediate footwall of the frontal thrust ramp, total shortening of the sedimentary cover ranges from 59 km (32%) for section B-B′ to 76 km (43%) for section E-E′. These values point out that there are no large differences in the total amount of shortening between northern and southern outer Albanides. The marked difference in structural style between the two regions is essentially controlled by detachment versus attachment of the Ionian basin succession in the southern and northern sectors, respectively. The restored sections of Figures 10 and 11 also show a general—though articulated (Table 1)—southward increasing original size of the Ionian basin, from 60 km (A-A′) to 132 km (E-E′).

A difference of shortening values between northern and southern outer Albanides characterizes also the basement, although the related thrust-related displacement measured along the sections (in the range of 5%–10%) is rather limited with respect to that of the overlying sedimentary cover (Table 1). This feature clearly implies substantial basement removal from the section by its ENE-ward translation, a process fully consistent with the general underthrusting of the Adria slab beneath the Dinarides-Albanides-Hellenides orogen (e.g., Cavazza & Wezel, 2003). For all the southern cross-sections (B-B′ to E-E′), the basement is substantially uplifted above regional in the frontal part of the fold and thrust belt. The interpretation proposed in the sections of Figures 10 and 11 involves the reverse-slip reactivation of inherited extensional faults originally bounding the Ionian basin. The role of a footwall shortcut in the basement (modeled by trishear as described in the previous section) is envisaged to have been particularly important in controlling the structural elevation of the Sazani units in the frontal part of the fold and thrust belt in sections B-B′, C-C′, and D-D′.

In order to provide a comprehensive picture of the tectonic evolution of the southern outer Albanides, sequential restoration of the sedimentary cover was coupled with forward modeling of the basement to display progressive fold and thrust belt development along a representative section (D-D′). Starting from the pre-orogenic template (stage 0), shortening is modeled as involving early fold amplification and subsequent break thrust propagation (mostly through the inflection separating the limbs of anticline-syncline pairs). In the forward model, coupled folding and break thrusting account for shortening of distinct rock volumes (areas in 2D) in a NE to SW progression within the framework of a foreland-ward migrating deformation. The proposed evolution is consistent with the regional constraints on the timing of the deformation provided by syn-tectonic deposits (e.g., Durmishi et al., 2014; and references therein). The early deformation stages (1 and 2 in Figure 12) involve the Cretaceous portion of the Kruja carbonate platform succession, which is detached along Lower Cretaceous evaporites and transported southwestward in the hanging wall of the Kruja thrust. Subsequent shortening of the Ionian basin succession is accommodated by folding and thrusting above the décollement level represented by the Triassic evaporites. This leads to the progressive development of the Berati belt (stages 2–6 in Figure 12) and then of the Kurvaleshi and Cika belts (stages 7–9 in Figure 13). Stages 10 and 11 (Figure 13) show the involvement in deformation of the Sazani carbonate platform succession, which is accompanied by basement faulting in the frontal part of the belt, leading to the present-day configuration (stage 12).

5. Discussion

Balanced and restored geological sections across the outer Albanides fold and thrust belt show a marked variation of structural style from the northern to the southern outer Albanides, particularly considering equivalent section segments including the Ionian and Sazani units (Figures 10 and 11). As it was already evident from seismic interpretation by Roure et al. (2004), the Ionian units appear not to be decoupled from the basement in the northern outer Albanides (section A-A′). On the other hand, in the southern outer Albanides (sections B-B′ to E-E′) the same units display a structural style strongly controlled by the occurrence of an efficient décollement level represented by the Triassic evaporites, whose great thickness is well documented in this sector of the belt (Frasheri

Figure 10. Balanced and restored geological sections across the northern and southern outer Albanides (located in Figures 3 and 5). No internal stratigraphy is shown for the Krasta-Cukali and Korabi tectonic units that are thrust on top of the outer units representing the subject of this study. Syn-tectonic strata are not included in the restorations, as these show the late Eocene setting. The balancing error is calculated for the sedimentary cover as the normalized difference between the longest and shortest horizons used in line-length balancing. The balancing error for each section is the following: A-A′ = 0.3%, B-B′ = 0.1%, and C-C′ = 0.3% (the variability of this value depends on section length and structural complexity). The basement of the Ionian basin is shown in a simplified fashion, since most extensional faults that likely affected it (Figure 4) are not imaged in seismic profiles. Dashed boxes show the location of the seismic profiles used in cross-section building. The focal mechanism for the M_w 6.4, 26 November 2019 earthquake (source: http://rcmt2.bo.ingv.it/; last access: 24 January 2022) is projected onto the vertical plane of section A-A′ at the proper hypocentral location.
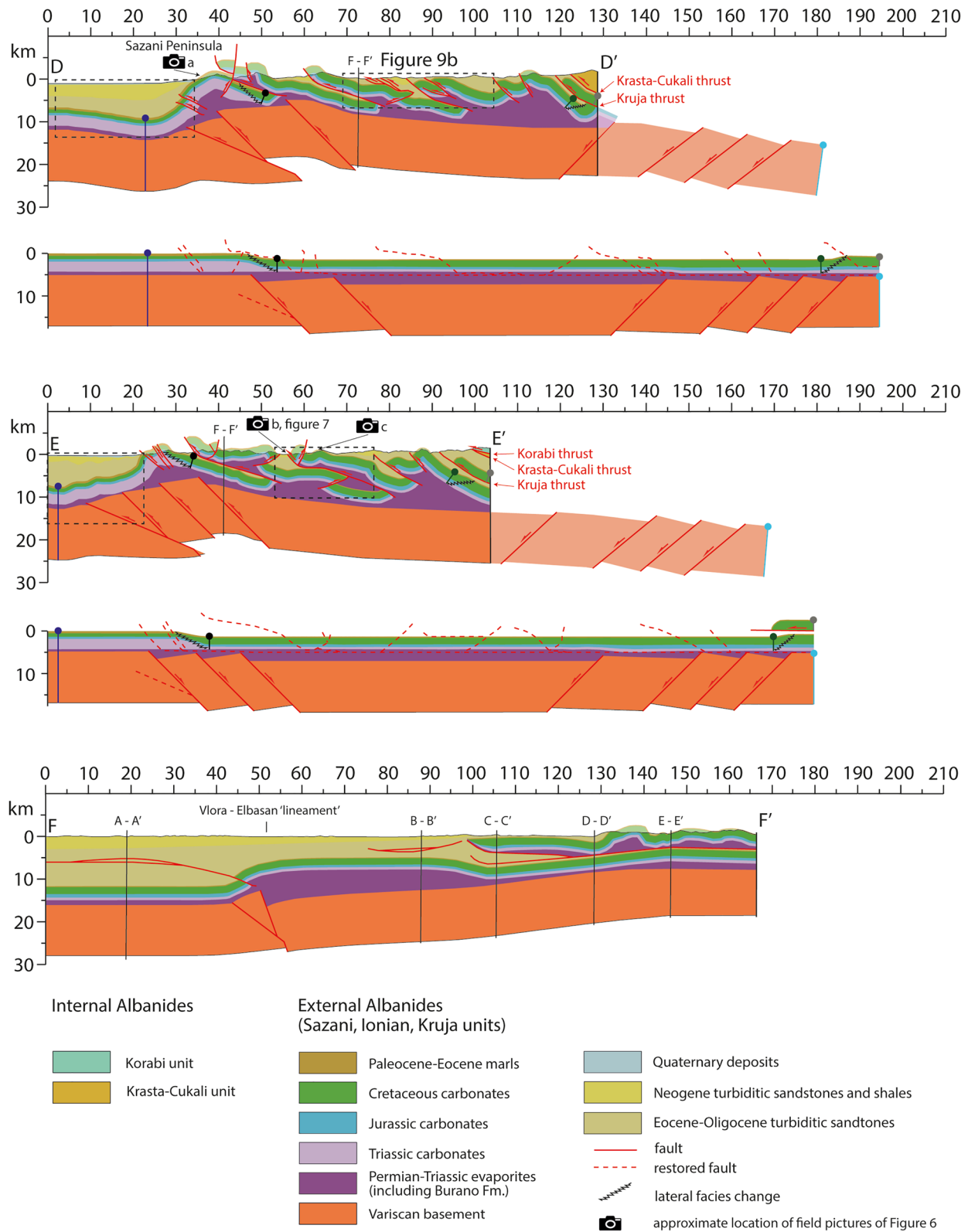
Figure 11. Balanced and restored geological sections across the southern outer Albanides, and NNW-SSE strike section (located in Figures 3 and 5). The balancing error for each dip section is the following: D-D′ = 0.5% and E-E′ = 0.1%. Dashed boxes show the location of the seismic profiles used in cross-section building.

Table 1
Deformed Lengths, Restored Lengths, and Shortening Values for the Balanced Geological Sections of This Study (the Values Were Measured Using Pin Lines Shown in Figures 10 and 11)

| Considered layer/tectonic unit	Restored length (km)	Final length (km)	Shortening (%)
Section A-A′			
Basement	113	107	5
Sedimentary cover	113	70	38
Ionian	60	59	2
Section B-B′			
Basement	186	167	10
Sedimentary cover	186	127	32
Ionian	125	77	38
Sazani + Ionian	175	123	30
Section C-C′			
Basement	181	162	10
Sedimentary cover	181	119	34
Ionian	128	73	43
Sazani + Ionian	172	112	35
Section D-D′			
Basement	171	158	8
Sedimentary cover	171	105	39
Ionian	127	72	43
Sazani + Ionian	158	100	37
Section E-E′			
Basement	177	166	6
Sedimentary cover	177	101	43
Ionian	132	71	54
Sazani + Ionian	167	74	44

et al., 2009; Velaj et al., 1999). Triassic evaporites are particularly thick in the Berati belt (Velaj, 2015b), where they also formed variable-sized diapirs (e.g., Lacombe et al., 2009; Robertson & Shallo, 2000; Velaj, 2001, 2015a). The largest of them, that is, the Dumre salt plug in central Albania (Figure 3), has been related with Mesozoic halokinesis (Bega & Soto, 2017; but see Jardin et al., 2011, for an alternative interpretation) largely affected by later thrust tectonics. Bega and Soto (2017) provided a detailed account of precursor salt pillows and salt walls that variably controlled later development of thrust-related structures. The cross-sections presented in this study follow the trace of seismic lines that do not cross salt diapirs documented by the latter authors. As the seismic lines used in this study do not show clear evidence of precursor salt-related deformation features, our structural interpretation (Figures 10 and 11) involves a pre-thrusting template not including salt diapirs. By no means this implies overlooking the importance of salt tectonics in the study area, which is clearly characterized by an articulated spatiotemporal distribution of salt diapirs and widespread salt flow. Structural development is shown in sections B-B′ to E-E′ as resulting from the SW-ward transport of faulted anticlines or fold trains in the hanging wall of break thrusts that locally accumulated relatively large displacements (of a few kilometers to >10 km; see, e.g., stages 9–10 in Figure 13). According to this interpretation, the thick décollement level represented by the Triassic evaporites played a major role in favoring buckling/detachment folding of the overlying carbonate succession. Following initial layer-parallel shortening (recorded by pressure-solution cleavage roughly perpendicular to bedding in competent limestone beds), break-thrust folds (Fischer et al., 1992) are envisaged to have evolved from an initial, brief stage of sinusoidal buckling to a later stage of fixed-hinge fold amplification and thrusting, leading to the development of fold-generated imbricates (Morley, 1994). The initial wavelength of such folds, involving multiple, evenly spaced, harmonically deforming layers, was probably controlled by the more competent "control units" represented by the Upper Triassic dolomite-Upper Cretaceous thick-bedded limestone couple. Overall bed thickness conservation in the Upper Triassic to Eocene carbonate multilayer (Figures 10–13) is consistent with the competent nature of these units, which involves the development of class 1B or class 1C folds (i.e., folds with no or only minor bed thickening in the hinge regions; Ramsay, 1967). Therefore, the concentric fold geometry that is generally dictated by algorithms in structural modeling software (Butler et al., 2019) is appropriate for the deformed competent multilayer of this study. This is clearly the case because concentric folding of the competent "control units" are accompanied by large thickness variations of the incompetent Triassic evaporites. Our kinematic model (Figures 12 and 13) is consistent with model outcomes showing the progressive development of fold-thrust systems characterized by a thick layer of very low-viscosity material at the base (Figure 14). According to Butler et al. (2019) such model outcomes are relevant for those fold-thrust belts that, similarly to the southern outer Albanides of this study, include thick evaporite layers at depth. Examples cited by this author are the Fars zone of the Zagros Mountains (e.g., Mouthereau et al., 2007) and the Provencal region of the Western Alps (Graham et al., 2012). In the model of Figure 14, fold amplification is accompanied by subsidence of synclinal troughs by withdrawal of incompetent material and its flow into to the core of the anticlines. This results in local significant thickening of the weak material in the latter structural positions, similarly to what is observed for the Triassic evaporites of our balanced sections B-B′ to E-E′ (Figures 10 and 11). In particular, the model of Figure 14 (30% shortening) would be comparable to stage 9 of the forward model in Figure 13.

Based on the foregoing discussion, it may be envisaged that a degraded quality of detachment resulted from the northward decreasing thickness of the Triassic evaporites, which was also likely accompanied by decreasing salt and gypsum components (Velaj, 2001). These stratigraphic variations were at least partly controlled by NE-SW striking basement faults that are presently marked by the transversal "lineaments" of the chain, particularly the
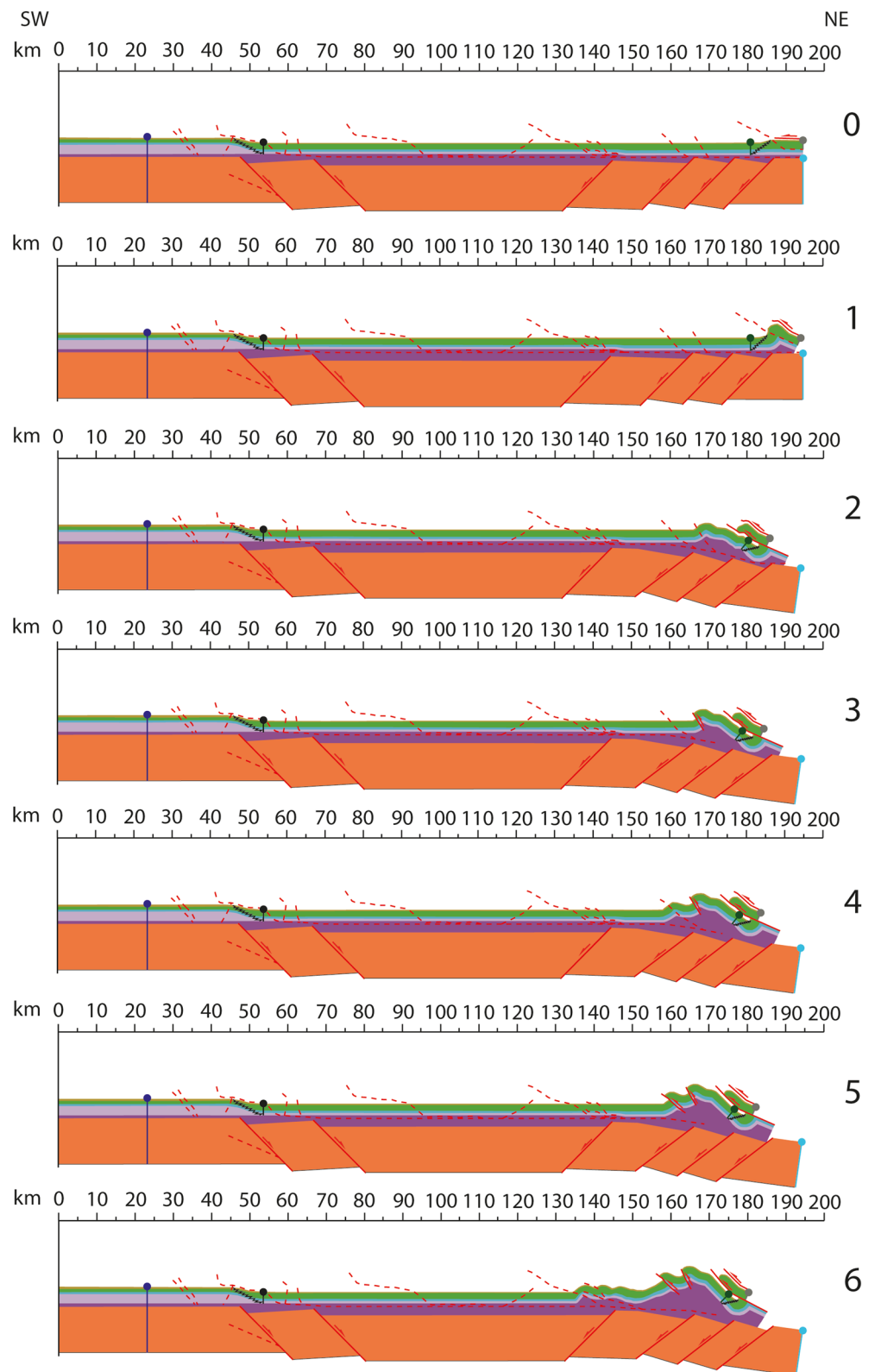
Figure 12. Early stages of fold and thrust belt development along section D-D′ integrating forward modeling of the basement and sequential restoration of the sedimentary cover. Area balancing was used to maintain the total amount of Triassic evaporites constant throughout the whole deformation sequence (although out-of-the section flow of salt could have occurred, this type of restoration is considered viable at the regional scale of the section; see text).
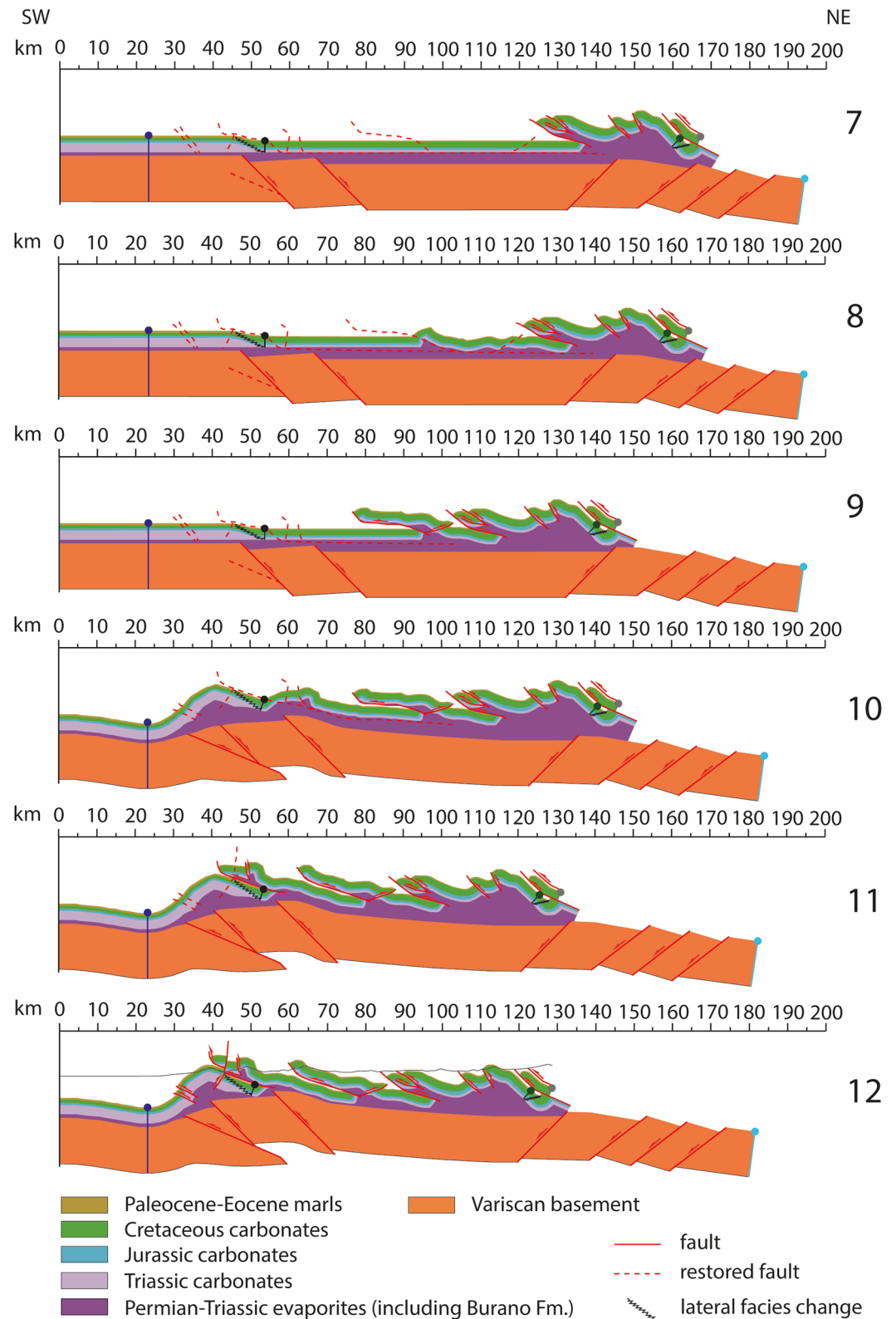
Figure 13. Late stages of fold and thrust belt development along section D-D′ integrating forward modeling of the basement and sequential restoration of the sedimentary cover.
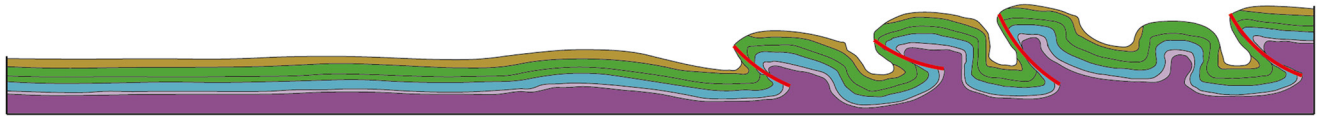
Figure 14. Results of numerical modeling by Simpson (2009, modified) showing fold-thrust system developed above a very low-viscosity décollement layer (30% shortening).

Vlora-Elbasan one (e.g., Durmishi et al., 2014; Lacombe et al., 2009; Nieuwland et al., 2001). The latter feature controlled the location of a major lateral ramp of the detachment-dominated thrust system, involving climbing of the basal décollement from the Triassic evaporites in the south to intra-Cenozoic overpressured shales in the north (Roure et al., 2004). This lateral ramp, depicted in section F-F′ in Figure 11, was active prior to late-stage basement-involved inversion (discussed below).

As it was described in the section dedicated to the restoration methods, area balancing of the Triassic evaporites was also used to integrate seismic interpretation to aid constraining underlying basement structures. This must be taken with caution, considering the uncertainties related with the three-dimensional nature of salt flow (e.g., Rowan & Ratliff, 2012; and references therein). In any case, fundamental information on basement-involved thrusting in the frontal part of the Albanides was provided by the previously mentioned seismological datasets related with the 2019–2020 Durrës seismic sequence (Teloni et al., 2021; Vittori et al., 2021). The major active upper crustal ramp shown in cross-section A-A′ (Figure 10) controls the blind thrust front in the northern outer Albanides. Upper crustal ramps—here footwall shortcuts associated with inversion structures—define the blind thrust front also in our sections B-B′ to E-E′ across the southern outer Albanides. Relatively large displacements along these basement faults account for the substantial structural elevation above regional of the Sazani units in the hanging wall of the frontal thrust in sections B-B′, C-C′, D-D′, and E-E′ (Figures 10 and 11). It is worth noting that even the basement of the Ionian basin succession (east of the Sazani units) is significantly elevated above regional due to the large vertical component of the reverse fault offset at the thrust front. On the other hand, the basement in the footwall of the thrust front lies at a depth of ∼12 km along the southernmost section (E-E′) and progressively deepens northward down to ∼20 km along section B-B′. This feature could be inherited from the Triassic architecture of the Ionian basin, which hosted a deeper salt basin south of the Vlora-Elbasan "lineament." Within this framework, it could be interpreted as the result of basement tilting in the hanging wall of a SE dipping Triassic normal fault. Along the northernmost section (A-A′), which is located in the original footwall block to this fault, the top basement rises back to ∼12 km at an equivalent structural position (i.e., in the immediate footwall of the thrust front).

Despite the originally deeper setting of the southern sector, here the basement beneath the detached and imbricated Ionian units lies at depths in the range of 5–13 km (sections B-B′ to E-E′). On the other hand, in the northern sector the top basement lies at a maximum depth in excess of 15 km beneath the—here attached—Ionian basin succession and the thick clastic fill of the Periadriatic Depression (section A-A′). These features indicate that the Ionian units in the southern sector of the chain were significantly uplifted and erosionally exhumed as a result of larger basement offset along the crustal ramp defining the thrust front. This is also reflected by the larger amounts of basement shortening in the southern sections with respect to the northern one (Table 1). These considerations point out that the Ionian basin sector located south of the Vlora-Elbasan "lineament" experienced a peculiar type of inversion, involving (a) a first stage of detachment-dominated thrusting and thickening of the sedimentary cover, which also reduced the accommodation space for syn-tectonic sediments; and (b) a later stage of crustal-scale inversion controlled by basement faulting, which further reduced the accommodation space for syn-tectonic sediments and eventually led to the emersion of the deformed Ionian basin succession. These processes were likely accompanied by the reactivation of the inherited basement fault underlying the Vlora-Elbasan "lineament." Assuming this fault was originally dipping to the SE, as discussed above, oblique-slip reactivation involving a reverse dip-slip component of motion would be consistent with uplift of the southern crustal block. This would have occurred within the framework of transpressional deformation along the boundary between the northern and southern crustal blocks. In Figure 11, the oblique inversion structure inferred along the Vlora-Elbasan "lineament" is hypothesized as involving a footwall shortcut (section F-F′).

According to Copley et al. (2009), the gravitational potential energy differences between the mountain chain of ENE Albania and the lowlands/offshore sectors to the WSW produced sub-parallel normal faulting and coeval

basement thrusting. In this model, the initiation of normal faulting in the belt interior was triggered by the reduced dimension of the topographic contrast that could be sustained by the western lowlands/submarine relief as a result of thermal weakening of the crust. Taking into account: (a) the latest Miocene to early Pliocene onset of extensional tectonics in the mountain chain of ENE Albania (Meco & Aliaj, 2000), and (b) the occurrence of an associated stage of significant exhumation at ∼4–6 Ma (Muceku et al., 2008), this model provides an approximate estimate of ∼5 Ma for the onset of basement involvement in deformation in the Albanides fold and thrust belt. It is worth noting that the envisaged tectonic evolution, characterized by late-stage basement thrusting in the frontal part of the chain, is common to other fold and thrust belts of the world (e.g., Tavani et al., 2021; and references therein). In particular, the process of upper crustal thrust ramp development in the outer Albanides is rather like that controlling the recent (<5 Ma) uplift of a prominent topographic feature—the Mountain Front Flexure—in the Lurestan sector of the Zagros Mountains (Basilici, 2020; Basilici et al., 2020; Emami et al., 2010; Homke et al., 2004; Koshnaw et al., 2017). Tavani et al. (2021) recently suggested that this process involves the reactivation of a middle crustal décollement originally located in the necking and proximal domains of the pre-existing passive continental paleomargin (Figure 2). In these domains, the middle crust retains its integrity during the rifting process, thereby providing an important mechanical weakness that may be re-used as a décollement during crustal shortening. On the other hand, the ductile middle crustal layer is largely disrupted in the hyperextended domain of the rifted margin due to intense stretching and thinning of the crust, thereby favoring thin-skinned thrusting during subsequent plate convergence. During this latter, the distal part of the rifted continental margin (Figure 4) arrives at the subduction zone after the complete consumption of the oceanic lithosphere. At this stage, the basal décollement propagates from the base of the ophiolitic sequences (Mirdita units in our instance) into the base of—or within—the sedimentary cover of the rifted margin. The involvement of continental extensional ribbons (such as the Kruja platform) does not appear to produce any remarkable effect on the detachment-dominated thrust system: the basal décollement remains confined to the sedimentary cover by shearing off the elevated plateaus (Tavani et al., 2021). When the original hyperextended domain of the down-going plate (i.e., the Ionian basin in southern Albania) arrives at the collision zone, shortening is still accommodated by detachment-dominated thrusting (Figure 2). This is shown by the Ionian basal décollement, which allowed folding and thrusting of the sedimentary succession of the distal portion of the rifted margin and its emplacement on top of the original proximal domain (i.e., the Sazani platform). As collision evolves, the basal décollement propagates from the hyperextended domain into the necking domain along weak stratigraphic levels (i.e., the thick Triassic evaporites of the Ionian basin in our instance). Further shortening and convergence reactivate the inherited middle crustal décollement and the overlying upper crustal faults of the necking and proximal domains (Figure 2). The Albanides case study suggests that collision-related thermal weakening of the crust—here documented by Copley et al. (2009)—plays a major role in the reactivation of the middle crustal décollement, thus providing a more general explanation for the late-orogenic basement involvement in deformation in the outer portions of fold and thrust belts.

5.1. Crustal Sections Across the Outer Albanides Fold and Thrust Belt

Crustal sections involving the occurrence of a middle crustal décollement in the outer Albanides are provided in Figure 15, based on the balanced sections A-A′ (Figure 10) and D-D′ (Figure 11) and available geophysical information on Moho geometry (Grad et al., 2009). Upper crustal thrust ramps (partly associated with inversion tectonics) in the frontal part of the belt are shown to splay out from the middle crustal décollement. Considering the previously discussed timing of basement involvement in deformation, late-orogenic reactivation of the middle crustal décollement shown in our balanced cross-sections would have occurred since ∼5 Ma as a result thermal weakening of the crust. This process has also major implications for the active tectonic setting of Albania: the demonstrated activity of frontal basement structures in the northern region indicates that aseismic shear strain accumulation along the middle crustal décollement triggers episodic seismic rupture of otherwise locked upper crustal faults splaying out from it, as it occurred during the 2019–2020 Durrës earthquake sequence (Teloni et al., 2021; Vittori et al., 2021). Recent crustal seismicity in the Greek offshore south of our study area suggests that active basement thrusting characterizes also the frontal part of the Hellenides fold and thrust belt (Kamberis et al., 2022, and references therein). Since active basement thrusts of the southern outer Albanides are not equally well constrained by recent seismicity, our crustal section D-D′ may be used (together with the other balanced sections of Figures 10 and 11) to model less known/elusive potential seismic sources. This, in turn, may have substantial implications for seismic hazard assessment in the densely populated region included in Figure 5.
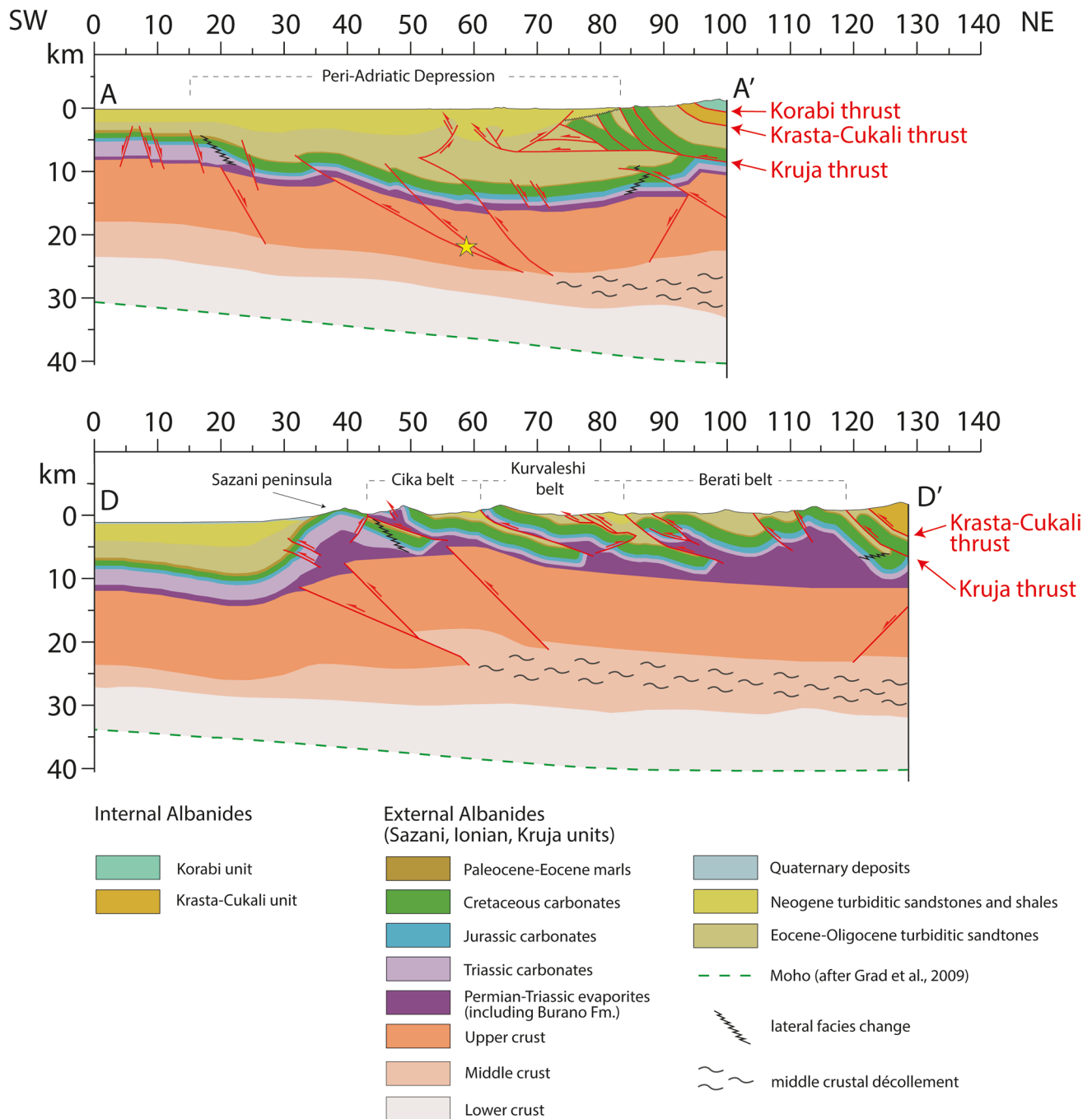
Figure 15. Crustal geological sections across the outer Albanides (section traces are located in Figure 3). No internal stratigraphy is shown for the Krasta-Cukali and Korabi tectonic units. Star shows hypocentral location of the M_w 6.4, 26 November 2019 earthquake (source: http://rcmt2.bo.ingv.it/; last access: 24 January 2022).

The cross-sections of Figure 15 highlight a fundamental difference in fold and thrust belt architecture between the northern and the southern outer Albanides. In the northern outer Albanides (section A-A′), a deep synformal foreland basin depocenter occurs in the footwall of the Kruja thrust; this depocenter constitutes the Peri-Adriatic Depression, which is filled by an up to 10 km thick Oligocene to Plio-Quaternary clastic succession. On the other hand, in the southern outer Albanides (section D-D′) the footwall of the Kruja thrust is "occupied" by imbricated Ionian basin units, which substantially reduced the accommodation space for syn-tectonic sediments.

Significant imbrication of the Kruja units and a relatively large Kruja thrust displacement characterize the northern section A-A′. This suggests that while folding and thrusting were effectively accommodating shortening of the Ionian sedimentary cover (soled by thick Triassic evaporites) to the south, the lack of an efficient décollement level at the base of the Ionian succession to the north favored additional slip accumulation along the Kruja thrust in its hanging wall (section A-A′ in Figure 15). The leading splay of the Kruja thrust propagated within the foredeep strata of the Peri-Adriatic Depression until it was eventually abandoned during the early Pliocene as deformation migrated at deeper crustal levels. The rapid accumulation of a huge thickness of syn-tectonic deposits, including on top of the frontal part of the thrust wedge, could have played an important role in arresting thin-skinned thrust propagation within the foreland basin succession. In fact, foredeep sedimentation is well known to produce perturbations of thrust belt propagation (e.g., Vergés & Muñoz, 1990). In our instance, the substantial amount of sediments that were deposited in the northern foreland basin, also burying the frontal part of the fold and thrust belt, could have eventually inhibited further thrust propagation within the foredeep. At the same time, these thick syn-tectonic deposits contributed to thermal weakening of the crust by providing a significant burial involving both radiogenic heat production within the sedimentary pile and a thermal blanketing effect (Copley et al., 2009). The combination of these processes is envisaged to have triggered a switch to ramp-dominated, basement-involved thrusting affecting the crustal segment hosting the Ionian basin. This is consistent with Lacombe and Bellahsen's (2016) observation that basement thrusting is favored in the outer portions of sediment-loaded orogens. In our study area, it resulted in the development of a new blind thrust front located within the Ionian basin succession (which is buried beneath the thick syn-tectonic succession of the Peri-Adriatic Depression).

Slowdown of thrust belt propagation affected also the southern outer Albanides as the thrust front reached the western margin of the Ionian basin and the eastern slope of the Sazani carbonate platform (stage 11 in Figure 13). Here, basement faults controlling the platform-to-basin transition and the reduced thickness of Triassic evaporites at the base of the Sazani platform succession are both likely to have significantly reduced the efficiency of the décollement. For this southern region, lacking the huge thickness of syn-tectonic strata accumulated in the Peri-Adriatic Depression to the north, a significant contribution to syn-collisional thermal weakening of the crust could be provided by intense imbrication and tectonic thickening of the detached sedimentary cover.

As detachment-dominated thrusting of the sedimentary cover was fading and eventually ceasing throughout the entire outer Albanides, the already mentioned thermal weakening of the orogenic crust favored a migration of the deformation at deeper structural levels. This process is inferred to have led to the reactivation of the inherited middle crustal décollement, which in turn triggered basement-involved thrusting during the last 5 Myr. The relatively low shortening values associated with basement thrusts in the outer Albanides (Table 1) are consistent with their recent activity, which postdated substantial Oligocene-Miocene deformation. Taking into account the previously discussed onset of basement deformation at ∼5 Ma, shortening rates of ∼1.2 (section A-A′) and ∼2.6 (section D-D′) mm year^{-1} are obtained for the northern and southern crustal sections, respectively. These values could be effectively compared with geodetic data made available by the permanent Global Navigational Satellite System (GNSS; stations were considered in the ETRF2000 "European fixed" reference frame; source: http://pnac.swisstopo.admin.ch/divers/dens_vel/combvel_se_all_cmb_grd_east.jpg; last access: 25 January 2022). The projection of displacement vectors from all GNSS stations located within 30 km from the trace of our cross-sections yielded mean foreland-ward motions of 1.5 ± 0.8 mm year^{-1} along A-A′ and of 2.5 ± 1.2 mm year^{-1} along D-D′ (a total of twelve stations—six for each section—fell within the threshold distance and were therefore considered in the analysis). Comparable long-term and short-term strain rates suggest a general steady-state deformation at the orogen scale during the last ∼5 Myr.

6. Concluding Remarks

Balanced and restored geological sections across the outer Albanides, despite outlining a marked difference in fold and thrust belt architecture between northern and southern segments, indicate that a switch from detachment-dominated thrusting of the sedimentary cover to ramp-dominated, basement-involved thrusting affected the whole fold and thrust belt. Regional geological and thermochronological constraints coupled with numerical modeling (Copley et al., 2009) suggest that basement involvement in deformation took place in the last ∼5 Myr as a result of thermal weakening of the crust. This latter process is interpreted to have led to the reactivation of an inherited (rifted margin-related) middle crustal ductile layer as a décollement level during the late

stages of fold and thrust belt development. Basement involvement in deformation (a) results in geological strain rate values that are generally consistent with geodetic ones, and (b) controls the active tectonic setting of the study area, which is characterized by earthquake nucleation within the crystalline upper crust.

Different processes appear to have concurred to slowdown and/or arrest detachment-dominated thrusting of the sedimentary cover. In the northern outer Albanides, the limited thickness of Triassic evaporites inhibited thrust belt propagation within the Ionian basin succession, favoring further advancement of the detached Kruja units in its hanging wall (refer to section A-A′ in Figure 15). The rapid accumulation of an up to 10 km thick succession of syn-tectonic strata in the Peri-Adriatic Depression likely had a twofold effect of: (a) stopping detachment-dominated thrust belt propagation into the foredeep strata, which was being accommodated by thrusts splaying out from the leading edge of the Kruja thrust; and (b) providing a burial that substantially contributed to thermal weakening of the crust. On the other hand, in the southern outer Albanides the Ionian basin carbonate succession, here overlying thick Triassic evaporites, was intensely shortened (refer to section D-D′ in Figure 15). Folding and detachment-dominated thrusting proceeded efficiently up to the western margin of the basin (Figure 13). There, normal faults controlling the platform-to-basin transition and the reduced thickness of the Triassic evaporites at the base of the Sazani carbonate platform succession hindered thrust belt propagation into the thick shallow-water carbonate succession. The latter was later broadly folded and significantly uplifted above regional by deformation associated with the crustal thrust ramp controlling the present-day blind thrust front in this southern sector of the belt. In this region, tectonic burial—produced by the imbricated and thickened sedimentary cover—rather than sedimentary burial likely contributed to thermal weakening of the crust. The final result all of these processes was the described major change in structural style that affected both the northern and southern regions of the outer Albanides.

At the crustal scale, stronger basin inversion in the southern External Albanides was essentially controlled by reverse slip along the frontal ramp located within the Sazani carbonate platform and underlying basement. This resulted in substantial uplift, erosion and related exhumation of the entire (Sazani-Ionian) outer segment of the fold and thrust belt. On the hand, in the northern External Albanides the thrust front is located more internally, within the Ionian basin succession (stratigraphically overlain by up to 10 km of syn-tectonic strata). Here limited reverse slip along the crustal ramp defining the thrust front did not produce significant basin inversion, and the top basement in its hanging wall remains at great depths (>15 km) within the flexural foreland basin forming the Periadriatic Depression (largely still submerged at present).

Although a late-stage switch from thin-skinned to thick-skinned thrusting has been documented in various fold and thrust belts around the world, the External Albanides case history sheds new light into the complex combination of geological factors that may control this process. Inherited (from the rifted continental margin) and syn-kinematic rheology, stratigraphy and structural features played different roles at various times and locations along the fold and thrust belt to produce the major changes in structural style documented in the outer Albanides. Cross-section balancing and restoration, constrained by good-quality subsurface data, confirmed to represent an irreplaceable tool to unravel the modes and timing of structural development in fold and thrust belts. This goes well beyond obtaining a mere—yet fundamental, as a starting point—"static" picture of fold and thrust belt architecture.

Data Availability Statement

The data supporting the interpretations and data products related to this paper are available in the Figshare repository: Albania—balanced and restored geological cross-sections. Journal contribution. https://doi.org/10.6084/m9.figshare.19180958.v4.

References

Anderson, H., & Jackson, J. (1987). Active tectonics of the Adrsiatic region. *Geophysical Journal International*, *91*(3), 937–983. https://doi.org/10.1111/j.1365-246X.1987.tb01675.x

Anelli, L., Gorza, M., Pieri, M., & Riva, M. (1994). Subsurface well data in the northern Apennines (Italy). *Memorie della Societa Geologica Italiana*, *48*, 461–471.

Ballard, J. F., Spina, V., Clément, F., Lardin, P. E., Moron, J. M., Fleury, J. M., & Chaffel, P. (2018). An integrated approach to de-risking exploration and appraisal in structurally complex fold-and-thrust belts: Application to the Incahuasi field (Bolivia). In G. Zamora, K. R.

McClay, & V. A. Ramos (Eds.), *Petroleum basins and hydrocarbon potential of the Andes of Peru and Bolivia*. AAPG Memoir. https://doi.org/10.1306/13622138M1173782

Bally, A. W., Burbi, L., Cooper, C., & Ghelardoni, R. (1986). Balanced sections and seismic reflection profiles across the Central Apennines. *Memorie della Societa Geologica Italiana*, *35*, 257–310.

Basilici, M. (2020). *Thermal structure and active tectonics of the frontal zone of the Zagros fold and thrust belt in Western Lurestan, Iran: New insights from 3-D geothermal analytical modelling and 2-D structural finite element modelling (doctoral dissertation)*. Università degli Studi di Urbino Carlo Bo. Retrieved from https://www.researchgate.net/publication/350838037_Thermal_Structure_and_Active_Tectonics_of_the_Frontal_Zone_of_the_Zagros_Fold_and_Thrust_Belt_in_Western_Lurestan_Iran_New_Insights_from_3-D_Geothermal_Analytical_Modelling_and_2-D_Structural_Finite_E

Basilici, M., Ascione, A., Megna, A., Santini, S., Tavani, S., Valente, E., & Mazzoli, S. (2020). Active deformation and relief evolution in the western Lurestan region of the Zagros mountain belt: New insights from tectonic geomorphology analysis and finite element modeling. *Tectonics*, *39*(12), e2020TC006402. https://doi.org/10.1029/2020TC006402

Bega, Z., & Soto, J. I. (2017). The ionian fold-and-thrust belt in Central and Southern Albania: A petroleum province with Triassic evaporites. In J. I. Soto, J. F. Flinch, & G. Tari (Eds.), *Permo-Triassic salt provinces of Europe, North Africa and the Atlantic Margins*. Elsevier. https://doi.org/10.1016/B978-0-12-809417-4.00025-2

Berberian, M. (1995). Master "blind" thrust faults hidden under the Zagros folds: Active basement tectonics and surface morphotectonics. *Tectonophysics*, *241*(3–4), 193–224. https://doi.org/10.1016/0040-1951(94)00185-C

Bortolotti, V., Kodra, A., Marroni, M., Mustafa, F., Pandolfi, L., Principi, G., & Saccani, E. (1996). Geology and petrology of ophiolitic sequences in the Mirdita region (northern Albania). *Ofioliti*, *21*, 3–20.

Butler, R. W. H., Bond, C. E., Cooper, M. A., & Watkins, H. (2018). Interpreting structural geometry in fold-thrust belts: Why style matters. *Journal of Structural Geology*, *114*, 251–273. https://doi.org/10.1016/j.jsg.2018.06.019

Butler, R. W. H., Bond, C. E., Cooper, M. A., & Watkins, H. (2019). Fold–thrust structures—Where have all the buckles gone? *Journal of the Geological Society*, *487*, 21–44. https://doi.org/10.1144/SP487.7

Butler, R. W. H., & Mazzoli, S. (2006). Styles of continental contraction: A review and introduction. In S. Mazzoli & R. W. H. Butler (Eds.), *Styles of continental contraction* (Vol. 414, pp. 1–10). Geological Society of America. https://doi.org/10.1130/2006.2414(01)

Butler, R. W. H., Mazzoli, S., Corrado, S., De Donatis, M., Di Bucci, D., Gambini, R., et al. (2004). Applying thick-skinned tectonic models to the Apennine thrust belt of Italy—Limitations and implications. In K. R. McClay (Ed.), *Thrust tectonics and hydrocarbon systems* (Vol. 82, pp. 647–667). AAPG Memoir.

Butler, R. W. H., Tavarnelli, E., & Grasso, M. (2006). Structural inheritance in mountain belts: An Alpine–Apennine perspective. *Journal of Structural Geology*, *28*(11), 1893–1908. https://doi.org/10.1016/j.jsg.2006.09.006

Castelluccio, A., Mazzoli, S., Andreucci, B., Jankowski, L., Szaniawski, R., & Zattin, M. (2016). Building and exhumation of the Western Carpathians: New constraints from sequentially restored, balanced cross sections integrated with low-temperature thermochronometry. *Tectonics*, *35*(11), 2698–2733. https://doi.org/10.1002/2016TC004190

Cavazza, W., & Wezel, C. (2003). The Mediterranean region—A geological primer. *Episodes*, *26*(3), 160–168. https://doi.org/10.18814/epiiugs/2003/v26i3/002

Chopin, C. (1987). Very-high-pressure metamorphism in the western Alps: Implications for subduction of continental crust. *Philosophical Transactions of the Royal Society A: Mathematical, Physical & Engineering Sciences*, *321*, 183–197. https://doi.org/10.1098/rsta.1987.0010

Cobbold, P. R. (1975). Fold propagation in single embedded layers. *Tectonophysics*, *27*(4), 333–351. https://doi.org/10.1016/0040-1951(75)90003-7

Cooper, M. A., & Trayner, P. M. (1986). Thrust-surface geometry: Implications for thrust-belt evolution and section-balancing techniques. *Journal of Structural Geology*, *8*(3–4), 305–312. https://doi.org/10.1016/0191-8141(86)90051-9

Copley, A., Boait, F., Hollingsworth, J., Jackson, J., & McKenzie, D. (2009). Subparallel thrust and normal faulting in Albania and the roles of gravitational potential energy and rheology contrasts in mountain belts. *Journal of Geophysical Research*, *114*(B5), B05407. https://doi.org/10.1029/2008JB005931

Coward, M. P. (1983). Thrust tectonics, thin skinned or thick skinned, and the continuation of thrusts to deep in the crust. *Journal of Structural Geology*, *5*(2), 113–123. https://doi.org/10.1016/0191-8141(83)90037-8

Coward, M. P., De Donatis, M., Mazzoli, S., Paltrinieri, W., & Wezel, F. C. (1999). Frontal part of the northern Apennines fold and thrust belt in the Romagna-Marche area (Italy): Shallow and deep structural styles. *Tectonics*, *18*(3), 559–574. https://doi.org/10.1029/1999TC900003

Curi, F. (1993). Oil generation and accumulation in the Albanide Ionian Basin. In A. M. Spencer (Ed.), *Generation, accumulation and production of Europe's hydrocarbons* (Vol. 3, pp. 281–293). Springer. https://doi.org/10.1007/978-3-642-77859-9_22

Decandia, F. A., Lazzarotto, A., Liotta, D., Cernobori, L., & Nicolich, R. (1998). The CROP03 traverse: Insights on post-collisional evolution of northern Apennines. *Memorie della Societa Geologica Italiana*, *52*, 427–439.

De Donatis, M., & Mazzoli, S. (1994). Kinematic evolution of thrust-related structures in the Umbro-Romagnan parautochthon (northern Apennines, Italy). *Terra Nova*, *6*, 563–574. https://doi.org/10.1111/j.1365-3121.1994.tb00523.x

Diamanti, F., Sadikaj, Y., Zaimi, L., Tushe, I., Gjoka, M., Prifti, I., & Murataj, B. (1995). Hydrocarbon potential of Albania. In *1965–1995, 30 years*. Albpetrol, Oil and Gas Institute.

Doglioni, C. (1995). Geological remarks on the relationships between extension and convergent geodynamic settings. *Tectonophysics*, *252*(1–4), 253–267. https://doi.org/10.1016/0040-1951(95)00087-9

Durmishi, Ç., Prifti, I., & Nazaj, S. (2014). Geodynamic Evolution, Petroleum Geology, Potential Source Rocks, Reservoirs, Seal Carbonate Sedimentary Systems, Ionian and Sazani Zones, Albania—Field Trip FT3. Tectonic Relationships between Ionian and Sazani Zones, Vlora Region, Albania—Field Trip FT4. In *Paper presented at the XX CBGA Congress, 24–26 September, Tirana, Albania*.

Egan, S. S., Kane, S., Budding, T. S., Williams, G. D., & Hodgetts, D. (1999). Computer modelling and visualisation of the structural deformation caused by movement along geological faults. *Computers & Geosciences*, *25*(3), 283–297. https://doi.org/10.1016/S0098-3004(98)00125-3

Emami, H., Vergés, J., Nalpas, T., Gillespie, P., Sharp, I., Karpuz, R., et al. (2010). Structure of the Mountain Front Flexure along Anaran anticline in the Pusht-e Kuh Arc (NW Zagros, Iran): Insights from sand box models. *Geological Society, London, Special Publications*, *330*(1), 155–178. https://doi.org/10.1144/SP330.9

Erslev, E. A. (1991). Trishear fault-propagation folding. *Geology*, *19*(6), 617–620. https://doi.org/10.1130/0091-7613(1991)019<0617:TFPF>2.3.CO;2

Fischer, M. P., Woodward, N. B., & Mitchell, M. M. (1992). The kinematics of break-thrust folds. *Journal of Structural Geology*, *14*(4), 451–460. https://doi.org/10.1016/0191-8141(92)90105-6

Frasheri, A., Bushati, S., & Bare, V. (2009). Geophysical outlook on structure of the Albanides. *Journal of the Balkan Geophysical Society*, *12*(1), 9–30. Retrieved from https://www.researchgate.net/publication/266565412_Gophysical_outlook_on_structure_of_the_Albanides

Frasheri, A., Nishani, P., Bushati, S., & Hyseni, A. (1996). Relationship between tectonic zones of the Albanides, based on results of geophysical studies. In P. Ziegler & F. Horvath (Eds.), *Structure and prospects of Alpine basins and forelands* (Vol. 170, pp. 485–511). Mémoire Museum national d'Histoire naturelle.

Giambiagi, L., Tunik, M., Ramos, V. A., & Godoy, E. (2009). The High Andean Cordillera of central Argentina and Chile along the Piuquenes Pass-Cordon del Portillo transect: Darwin's pioneering observations compared with modern geology. *Revista de la Asociación Geológica Argentina*, *64*(1), 43–54.

Gibbs, A. D. (1983). Balanced cross-section construction from seismic sections in areas of extensional tectonics. *Journal of Structural Geology*, *5*(2), 153–160. https://doi.org/10.1016/0191-8141(83)90040-8

Grad, M., Tiira, T., & Working Group, E. S. C. (2009). The Moho depth map of the European Plate. *Geophysical Journal International*, *176*(1), 279–292. https://doi.org/10.1111/j.1365-246X.2008.03919.x

Graham, R. H., Jackson, M., Pilcher, R., & Kilsdonk, B. (2012). Allochthonous salt in the sub-Alpine fold–thrust belt of Haure Provence, France. In G. I. Alsop, S. G. Archer, A. J. Hartley, N. T. Grant, & R. Hodgekinson (Eds.), *Salt tectonics, sediments and prospectivity* (Vol. 363, pp. 595–615). Geological Society, London, Special Publications. https://doi.org/10.1144/SP363.30

Hatziyannis, G., Falus, G., Georgiev, G., & Sava, C. (2009). Assessing capacity for geological storage of carbon dioxide in central–east group of countries (EU GeoCapacity project). *Energy Procedia*, *1*(1), 3691–3697. https://doi.org/10.1016/j.egypro.2009.02.167

Homke, S., Vergés, J., Garcés, M., Emami, H., & Karpuz, R. (2004). Magnetostratigraphy of Miocene-Pliocene Zagros foreland deposits in the front of the Push-e Kush arc (Lurestan Province, Iran). *Earth and Planetary Science Letters*, *225*(3–4), 397–410. https://doi.org/10.1016/j.epsl.2004.07.002

Jamison, W. R. (1987). Geometric analysis of fold development in over thrust terranes. *Journal of Structural Geology*, *9*(2), 207–219. https://doi.org/10.1016/0191-8141(87)90026-5

Jardin, A., Roure, F., & Nikolla, L. (2011). Subsalt depth seismic imaging and structural interpretation in Dumre Area, Albania. *Oil and Gas Science and Technology*, *66*(6), 911–929. https://doi.org/10.2516/ogst/2011100

Kamberis, E., Kokinou, E., Koci, F., Lioni, K., Alves, T. M., & Velaj, T. (2022). Triassic evaporites and the structural architecture of the external Hellenides and Albanides (SE Europe): Controls on the petroleum and geoenergy systems of Greece and Albania. *International Journal of Earth Sciences*, *111*(3), 789–821. https://doi.org/10.1007/s00531-021-02151-4

Kane, S. J., Williams, G. D., Buddin, T. S., Egan, S. S., & Hodgetts, D. (1997). Flexural-slip based restoration in 3D, a new approach. In *Paper presented at the AAPG Annual Convention, 6–9 April, Dallas, Texas*.

Kodra, A., Gjata, K., & Bakalli, F. (1993). Les principales etapes de l'evolution paleogeographique et geodynamique des Albanides internes au cours du Mesozoique. *Bulletin de la Societe Geologique de France*, *164*(1), 69–77.

Kodra, A., Vergely, P., Gjata, K., Bakalli, F., & Godroli, M. (1993). La formation volcano-sedimentaire du Jurassique superieur; temoin de l'ouverture du domaine ophiolitique dans les Albanides internes. *Bulletin de la Societe Geologique de France*, *164*(1), 61–67.

Koshnaw, R. I., Horton, B. K., Stockli, D. F., Barber, D. E., Tamar-Agha, M. Y., & Kendall, J. J. (2017). Neogene shortening and exhumation of the Zagros fold-thrust belt and foreland basin in the Kurdistan region of northern Iraq. *Tectonophysics*, *694*, 332–355. https://doi.org/10.1016/j.tecto.2016.11.016

Lacombe, O., & Bellahsen, N. (2016). Thick-skinned tectonics and basement-involved fold-thrust belts: Insights from selected Cenozoic orogens. *Geological Magazine*, *153*(5/6), 763–810. https://doi.org/10.1017/S0016756816000078

Lacombe, O., Malandain, J., Vilasi, N., Amrouch, K., & Roure, F. (2009). From paleostresses to paleoburial in fold–thrust belts: Preliminary results from calcite twin analysis in the Outer Albanides. *Tectonophysics*, *475*(1), 128–141. https://doi.org/10.1016/j.tecto.2008.10.023

Manatschal, G. (2004). New models for evolution of magma-poor rifted margins based on a review of data and concepts from West Iberia and the Alps. *International Journal of Earth Sciences*, *93*(3), 432–466. https://doi.org/10.1007/s00531-004-0394-7

Mazzoli, S., Ascione, A., Buscher, J. T., Pignalosa, A., Valente, E., & Zattin, M. (2014). Low-angle normal faulting and focused exhumation associated with late Pliocene change in tectonic style in the southern Apennines (Italy). *Tectonics*, *33*(9), 1802–1818. https://doi.org/10.1002/2014TC003608

Mazzoli, S., Barkham, S., Cello, G., Gambini, R., Mattioni, L., Shiner, P., & Tondi, E. (2001). Reconstruction of continental margin architecture deformed by the contraction of the Lagonegro Basin, southern Apennines, Italy. *Journal of the Geological Society*, *158*(2), 309–319. https://doi.org/10.1144/jgs.158.2.309

McClay, K. R. (1992). Glossary of thrust tectonics terms. In K. R. McClay (Ed.), *Thrust tectonics*. Chapman & Hall.

McNaught, M. A., & Mitra, G. (1993). A kinematic model for the origin of footwall synclines. *Journal of Structural Geology*, *15*(6), 805–808. https://doi.org/10.1016/0191-8141(93)90064-H

Mecaj, B., & Mahmutaj, L. (1995). The main lithologo-petrographic characteristics of carbonate and terrigenous deposits in the south-western external Albanides. In *Paper presented at the ALBPETROL-95 Symposium, 24–26 September, Fier, Albania*.

Meco, S., & Aliaj, S. (2000). *Geology of Albania, Beiträge zur regionalen Geologie der Erde*. Gebrueder Borntraeger.

Morley, C. K. (1994). Fold-generated imbricates: Examples from the Caledonides of southern Norway. *Journal of Structural Geology*, *16*(5), 619–631. https://doi.org/10.1016/0191-8141(94)90114-7

Mouthereau, F., Lacombe, O., Tensi, J., Bellahsen, N., Kargar, S., & Amrouch, K. (2007). Mechanical constraints on the development of the Zagros Folded Belt (Fars). In O. Lacombe, J. Lavé, F. Roure, & J. Vergés (Eds.), *Thrust belts and foreland basins: From fold kinematics to hydrocarbon systems* (pp. 247–266). Springer. https://doi.org/10.1007/978-3-540-69426-7_13

Muceku, B., Mascle, G. H., & Tashko, A. (2006). First results of fission-track thermochronology in the Albanides. *Journal of the Geological Society*, *260*, 539–556. https://doi.org/10.1144/GSL.SP.2006.260.01.23

Muceku, B., van der Beek, P., Bernet, M., Reiners, P., Mascle, G., & Tashko, A. (2008). Thermochronological evidence for Mio-Pliocene late orogenic extension in the north-eastern Albanides (Albania). *Terra Nova*, *20*(3), 180–187. https://doi.org/10.1111/j.1365-3121.2008.00803.x

Nieuwland, D. A., Oudmayer, B. C., & Valbona, U. (2001). The tectonic development of Albania: Explanation and prediction of structural styles. *Marine and Petroleum Geology*, *18*(1), 161–177. https://doi.org/10.1016/S0264-8172(00)00043-X

Pfiffner, O. A. (2006). Thick-skinned and thin-skinned styles of continental contraction. In S. Mazzoli & R. W. H. Butler (Eds.), *Styles of continental contraction* (Vol. 414, pp. 153–177). Geological Society of America. https://doi.org/10.1130/2006.2414(09)

Pfiffner, O. A. (2017). Thick-skinned and thin-skinned tectonics: A global perspective. *Geosciences*, *7*(3), 71. https://doi.org/10.3390/geosciences7030071

Prenjasi, E., Karriqi, A., Nazaj, S., & Gjoni, K. (2011). Tectonic setting and hydrocarbon potential of theAlbanides fold-and-thrust belts. In *Paper presented at the 17th Meeting of the Association of European Geological Societes, 14–18 September, Belgrade, Serbia*.

Price, N. J., & Cosgrove, J. W. (1990). *Analysis of geological structures*. Cambridge University Press.

Proietti, G., Cvetković, M., Saftić, B., Conti, A., Romano, V., & Bigi, S. (2021). 3D modelling and capacity estimation of potential targets for CO_2 storage in the Adriatic Sea, Italy. *Petroleum Geoscience*, *28*(1), 117. https://doi.org/10.1144/petgeo2020-117

Ramsay, J. G. (1967). *Folding and fracturing of rocks*. McGraw-Hill.

Ramsay, J. G. (1981). Tectonics of the Helvetic Nappes. *Journal of the Geological Society*, *9*, 293–309. https://doi.org/10.1144/GSL. SP.1981.009.01.26

Ramsay, J. G. (1992). Some geometric problems of ramp-flat thrust models. In K. R. McClay (Ed.), *Thrust tectonics*. Chapman & Hall.

Ramsay, J. G., & Huber, M. I. (1987). The techniques of modern structural geology. In *Folds and fractures* (Vol. 2, p. 391). Academic Press. https://doi.org/10.1017/S0016756800010384

Robertson, A., & Shallo, M. (2000). Mesozoic–Tertiary tectonic evolution of Albania in its regional Eastern Mediterranean context. *Tectonophysics*, *316*(3–4), 197–254. https://doi.org/10.1016/S0040-1951(99)00262-0

Roure, F., Fili, I., Nazaj, S., Cadet, J. P., Mushka, K., & Bonneau, M. (2004). Kinematic evolution and petroleum systems-an appraisal of the outer Albanides. In K. R. McClay (Ed.), *Thrust tectonics and hydrocarbon systems* (Vol. 82, pp. 474–493). AAPG Memoir. https://doi.org/10.1306/M82813C25

Roure, F., Prenjasi, E., & Xhafa, Z. (1995). Petroleum geology of the Albanian thrust belt—Guide book to the Field Trip 7. In *Paper presented at the AAPG International Conference, 10–13 September, Nice, France*.

Roure, F., & Sassi, W. (1995). Kinematics of deformation and petroleum system appraisal in Neogene foreland fold-and-thrust belts. *Petroleum Geoscience*, *1*(3), 253–269. https://doi.org/10.1144/petgeo.1.3.253

Rowan, M. G., & Ratliff, R. A. (2012). Cross-section restoration of salt-related deformation: Best practices and potential pitfalls. *Journal of Structural Geology*, *41*, 24–37. https://doi.org/10.1016/j.jsg.2011.12.012

Rubert, Y., Jati, M., Loisy, C., Cerepi, A., Foto, G., & Muska, K. (2012). Sedimentology of resedimented carbonates: Facies and geometrical characterisation of an upper Cretaceous calciturbidite system in Albania. *Sedimentary Geology*, *257–260*, 63–77. https://doi.org/10.1016/j.sedgeo.2012.02.009

Saccani, E., Dilek, Y., & Photiades, A. (2017). Time-progressive mantle-melt evolution and magma production in a Tethyan marginal sea: A case study of the Albanide-Hellenide ophiolites. *Lithospere*, *10*(1), 35–53. https://doi.org/10.1130/L602.1

Santini, S., Basilici, M., Invernizzi, C., Mazzoli, S., Megna, A., Pierantoni, P. P., et al. (2020). Thermal structure of the northern outer Albanides and adjacent adriatic crustal sector, and implications for geothermal energy systems. *Energies*, *13*(22), 6028. https://doi.org/10.3390/en13226028

Scisciani, V. (2009). Styles of positive inversion tectonics in the Central Apennines and in the Adriatic foreland: Implications for the evolution of the Apennine chain (Italy). *Journal of Structural Geology*, *31*(11), 1276–1294. https://doi.org/10.1016/j.jsg.2009.02.004

Seeber, L., Armbruster, G., & Quittmeyer, R. C. (1981). Seismicity and continental subduction in the Himalayan arc. In H. K. Gupta & F. M. Delany (Eds.), *Zagros, Hindu Kush, Himalaya Geodynamic Evolution, Geodynamics Series* (Vol. 4, pp. 215–242). American Geographical Union. https://doi.org/10.1029/GD003p0215

Sepehr, M., & Cosgrove, J. W. (2004). Structural framework of the Zagros fold-thrust belt, Iran. *Marine and Petroleum Geology*, *21*(7), 829–843. https://doi.org/10.1016/j.marpetgeo.2003.07.006

Shehu, H. (1995). The geological feature and oil and gas bearing perspective of Kruja tectonic zone. In *Paper presented at the ALBPETROL-95 Symposium, 24–26 September, Fier, Albania*.

Simpson, D. D. H. (2009). Mechanical modelling of folding versus faulting in brittle–ductile wedges. *Journal of Structural Geology*, *31*, 369–381.

Tavani, S., Camanni, G., Nappo, M., Snidero, M., Ascione, A., Valente, E., et al. (2020). The Mountain Front Flexure in the Lurestan region of the Zagros belt: Crustal architecture and role of structural inheritances. *Journal of Structural Geology*, *135*, 104022. https://doi.org/10.1016/j.jsg.2020.104022

Tavani, S., Granado, P., Corradetti, A., Camanni, G., Vignaroli, G., Manatschal, G., et al. (2021). Rift inheritance controls the switch from thin- to thick-skinned thrusting and basal décollement re-localization at the subduction-to-collision transition. *GSA Bulletin*, *133*(9–10), 2157–2170. https://doi.org/10.1130/B35800.1

Tavani, S., Parente, M., Puzone, F., Corradetti, A., Gharabeigli, G., Valinejad, M., et al. (2018). The seismogenic fault system of the 2017 M_w 7.3 Iran–Iraq earthquake: Constraints from surface and subsurface data, cross-section balancing, and restoration. *Journal of Geophysical Research: Solid Earth*, *9*(3), 821–831. https://doi.org/10.5194/se-9-821-2018

Tavani, S., Parente, M., Vitale, S., Iannace, A., Corradetti, A., Bottini, C., et al. (2018). Early Jurassic rifting of the Arabian passive continental margin of the Neo-Tethys. Field evidence from the Lurestan region of the Zagros fold-and-thrust belt, Iran. *Tectonics*, *37*(8), 2586–2607. https://doi.org/10.1029/2018TC005192

Teloni, S., Invernizzi, C., Mazzoli, S., Pierantoni, P. P., & Spina, V. (2021). Seismogenic fault system of the M_w 6.4 November 2019 Albania earthquake: New insights into the structural architecture and active tectonic setting of the outer Albanides. *Journal of the Geological Society, London*, *178*(2), 193. https://doi.org/10.1144/jgs2020-193

Tremblay, A., Meshi, A., Deschamps, T., Goulet, F., & Goulet, N. (2015). The Vardar zone as a suture for the Mirdita ophiolites, Albania: Constraints from the structural analysis of the Korabi-Pelagonia zone. *Tectonics*, *34*(2), 352–375. https://doi.org/10.1002/2014TC003807

Turcotte, D., & Schubert, G. (2014). *Geodynamics* (3rd ed.). Cambridge University Press.

van Hinsbergen, D. J. J., Trond, H. T. H., Schmid, S. M., Liviu, C. M., Maffione, M., Visser, R. L. M., et al. (2020). Orogenic architecture of the Mediterranean region and kinematic reconstruction of its tectonic evolution since the Triassic. *Gondwana Research*, *81*, 79–229. https://doi.org/10.1016/j.gr.2019.07.009

Velaj, T. (2001). Evaporite in Albania and their impact on the thrusting processes. *Journal of the Balkan Geophysical Society*, *4*(1), 9–18.

Velaj, T. (2011). Tectonic style in Western Albania Thrustbelt and its implication on hydrocarbon exploration. In *Paper presented at the AAPG International Convention and Exhibition, 23–26 October, Milan, Italy*.

Velaj, T. (2015a). New ideas on the tectonic of the Kurvaleshi anticlinal belt in Albania, and the perspective for exploration in its subthrust. *Petroleum*, *1*(4), 269–288. https://doi.org/10.1016/j.petlm.2015.10.013

Velaj, T. (2015b). The structural style and hydrocarbon exploration of the subthrust in the Berati Anticlinal Belt, Albania. *Journal of Petroleum Exploration and Production Technology*, *5*(2), 123–145. https://doi.org/10.1007/s13202-015-0162-1

Velaj, T., Davison, I., Serjani, A., & Alsop, I. (1999). Thrust tectonics and the role of evaporites in the Ionian zone of the Albanides. *AAPG Bulletin*, *83*(9), 1408–1425. https://doi.org/10.1306/E4FD41CF-1732-11D7-8645000102C1865D

Vergely, P., Ardiana, D., & Patrik, M. (1998). Datation des semelles métamorphiques ophiolitiques d'Albanie par la méthode 40Ar/39Ar: Conséquences sur le mécanisme de leur mise en place40Ar/39Ar dating of metamorphic soles from the Albanian ophiolites: Implications for their emplacement models. *Comptes Rendus de l'Academie des Sciences: Series II A: Earth and Planetary Science*, *326*(10), 717–722. https://doi.org/10.1016/S1251-8050(98)80183-3

Vergés, J., & Muñoz, J. A. (1990). Thrust sequence in the southern central Pyrenees. *Bulletin de la Societe Geologique de France*, *6*(2), 265–271. https://doi.org/10.2113/gssgfbull.VI.2.265

Vergés, J., Saura, E., Casciello, E., Fernàndez, M., Villaseñor, A., Jiménez-Munt, I., & Garcìa-Castellanos, D. (2011). Crustal-scale cross-sections across the NW Zagros belt: Implications for the Arabian margin reconstruction. *Geological Magazine*, *148*(5–6), 739–761. https://doi.org/10.1017/S0016756811000331

Verrall, P. (1981). *Structural interpretation with applications to North Sea problems*. Joint Association for Petroleum Exploration Courses (UK).

Verwater, V. F., Le Breton, E., Handy, M. R., Picotti, V., Najafabadi, A. J., & Haberland, C. (2021). Neogene kinematics of the Giudicarie Belt and eastern Southern Alpine orogenic front (northern Italy). *Journal of Geophysical Research: Solid Earth*, *12*(6), 1309–1334. https://doi.org/10.5194/se-12-1309-2021

Vilasi, N. (2009). *Study of reservoir analogues in foreland fold-and-thrust belts: Sedimentology, diagenesis, deformation and fracturing of the upper cretaceous-eocene carbonate systems of the ionian zone (southern Albania) (Doctoral dissertation)*. École Nationale Supérieure des Mines de Paris, Sciences of the Universe [physics]. Retrived from https://pastel.archives-ouvertes.fr/pastel-00006128

Vilasi, N., Malandain, J., Barrier, L., Callot, J. P., Amrouch, K., Guilhaumou, N., et al. (2009). From outcrop and petrographic studies to basin-scale fluid flow modelling: The use of the Albanian natural laboratory for carbonate reservoir characterisation. *Tectonophysics*, *474*(1–2), 367–392. https://doi.org/10.1016/j.tecto.2009.01.033

Viti (2014). *Harta Gjeologjike Qarku Gjirokaster (scale 1:100,000)*. Ministria e Energjisë dhe Industrisë Shërbimi Gjeologjik Shqiptar, Drejtoria e Përgjithshme.

Vittori, E., Blumetti, A. M., Comerci, V., Di Manna, P., Piccardi, L., Gega, D., & Hoxha, I. (2021). Geological effects and tectonic environment of the 26 November 2019, M_w 6.4 Durres earthquake (Albania). *Geophysical Journal International*, *225*(2), 1174–1191. https://doi.org/10.1093/gji/ggaa582

Whitmarsh, R., Manatschal, G., & Minshull, T. (2001). Evolution of magma-poor continental margins from rifting to seafloor spreading. *Nature*, *413*(6852), 150–154. https://doi.org/10.1038/35093085

Withjack, M. O., & Peterson, E. T. (1993). Prediction of normal fault geometries—A sensitivity analysis. *AAPG Bulletin*, *77*, 1860–1873.

Xhomo, A., Kodra, A., Shallo, M., & Xhafa, Z. (2002). *Geology of Albania and geological map (scale 1:200,000)*. Geological Survey of Albania.

Zappaterra, E. (1990). Carbonate paleogeographic sequences of the Periadriatic region. *Bollettino della Societa Geologica Italiana*, *109*, 5–20.

Zappaterra, E. (1994). Source-rock distribution of the Periadriatic region. *AAPG Bulletin*, *78*, 333–354.